Differentiability at the Tip of Arnold Tongues for Diophantine Rotations: Numerical Studies and Renormalization Group Explanations

Rafael de la Llave · Alejandro Luque

Received: 5 July 2010 / Accepted: 20 May 2011 / Published online: 2 June 2011 © Springer Science+Business Media, LLC 2011

Abstract We study numerically the regularity of Arnold tongues corresponding to Diophantine rotation numbers of circle maps at the edge of validity of KAM theorem. This serves as a good test for the numerical stability of two different algorithms. We find empirically that Arnold tongues are only finitely differentiable at the tip. We also find several scaling properties of the Sobolev norms of the conjugacy near the breakdown. We also provide a renormalization group explanation of the regularity at the tip and the scaling behaviors of the Sobolev regularity. We also uncover empirically some other patterns which require explanation.

Keywords Arnold tongues · Renormalization · Scaling properties · Computational methods

1 Introduction

The study of circle maps was initiated by Poincaré in [41], motivated by Celestial Mechanics more than a century ago, and has been an active area of both theoretical and applied research. Circle maps arise in many other applications (the reader interested in examples of such applications is referred to [15, 22, 27, 39, 42]).

An important topological invariant for circle maps is the rotation number (see Definition 2.1) and, given a two-parametric family of circle maps, the set of parameters for which the rotation number takes a prefixed value is called Arnold tongue (some authors prefer to reserve the name "tongue" for rational values only). KAM theory—we refer to Sect. 2 for

R. de la Llave

Department of Mathematics, University of Texas at Austin, University Station C1200, Austin, TX 78712-0257, USA

e-mail: llave@math.utexas.edu

A. Luque (⊠)

Departament de Matemàtica Aplicada I, Universitat Politècnica de Catalunya, Diagonal 647, 08028 Barcelona, Spain

e-mail: alejandro.luque@upc.edu



precise definitions, statements and references—shows that, for analytic families of analytic circle maps satisfying some mild non-degeneracy conditions, the Arnold tongue corresponding to a Diophantine rotation number (see Definition 2.2) is an analytic curve. This result does not give any information if the family includes some subfamily for which the maps are analytic but have a critical value.

The goal of this paper is to study numerically the differentiability at the boundary (critical value) of Arnold tongues corresponding to Diophantine rotation numbers and to present a renormalization group explanation of the phenomena encountered. In particular, we show that Arnold tongues are at least $\mathcal{C}^{1+\alpha}$ at the critical point and we also predict which is (generically) the regularity of the tongues at this value using renormalization group arguments.

Our numerical study is performed using two different numerical methods. Both methods are solidly build, in the sense that there is a mathematical theory that validates the results obtained. In addition, both methods take advantage of the geometry and the dynamics of the problem to exploit cancellations that reduce the operation count and the storage requirements. For this reason the algorithms we present are reliable as well as efficient. It is quite encouraging that, even if the algorithms are so different, they produce results which agree with 8–10 figures.

- Firstly, a method for computing Diophantine rotation numbers of circle diffeomorphisms has been introduced in [46] and later extended in [35] to obtain derivatives with respect to parameters. This method consists in averaging the iterates of the map (or their derivatives) together with Richardson extrapolation.
- Secondly, we present a numerical algorithm, based on ideas introduced in [37, 38] and further developed in [59, 60], to compute Diophantine Arnold tongues. The papers above, showed that using the group structure of the problem, one can obtain a quasi-Newton method to solve a difference equation. We remark that, with appropriate choices of discretizations and algorithms, one can implement this quasi-Newton method in a fast way. Basically, if we keep at the same time a space discretization and Fourier discretization, the quasi-Newton method reduces to steps that are diagonal either in Fourier space or in real space. We observe that this method gives us the Fourier coefficients of the conjugacy, so that we can study its Sobolev norms, which we will see, give valuable information about the breakdown.

It is worth mentioning that both methods are designed to perform efficient computations for non-critical maps. For this reason, approaching critical values of the parameters is a good test for the behavior of the algorithms at their limit of validity. Moreover, as a consequence of the fact that Arnold tongues are differentiable at the critical point (see Proposition 5.1) we can compute critical values by extrapolation, thus obtaining higher precision than the one given by the method in [16, 47].

Renormalization group and scaling ideas provide powerful tools for the study of long term dynamics, supported by the fact that highly iterated maps, when observed in small scales, have forms that are largely independent of the map. These methods were first introduced in dynamical systems for unimodal maps [19, 52]. Later, numerical works in [21, 47] revealed that cubic critical circle maps exhibit interesting "universal" properties, very similar to those of phase transitions. From the point of view of rigorous mathematical foundations, many efforts have been made to develop a renormalization group theory that explains the observed properties (we refer to [8, 18, 33, 40, 48, 49, 54, 55]). The references just mentioned provide different rigorous formalisms which are better or worse suited depending on the context of study. For convenience, we shall use either of the different approaches according to our needs.



We emphasize that we present the renormalization group picture at the level of rigor usual in theoretical physics and we omit several precisions (complete specification of the Banach manifolds, descriptions of the domains etc.) needed for a fully mathematical formulation. We, of course, believe that such precisions are important, and we hope to come back to them. Since this paper is somewhat long already, we decided to concentrate in numerical algorithms and the phenomena they uncover. Other (important!) precisions that adhere to different standards will be dealt with elsewhere. We note that the rigorous definitions of renormalization are much easier in dynamical systems than in statistical mechanics or field theory.

To prove differentiability of Arnold tongues at the critical point, we study scaling relations of the derivatives of the rotation number with respect to parameters using cumulant operators. To this end we apply results reported in [5, 6]. It turns out that the asymptotic properties of cumulant operators characterize the growth of the different derivatives of the rotation number (see Proposition 5.1). This allows us to control the first derivative of Arnold tongues.

To establish a bound for the borderline regularity of an Arnold tongue, we give an explanation of the observed phenomenon based on a renormalization group picture. In this well-known picture, there is a non-trivial (universal) critical point having stable and unstable invariant manifolds that organize the dynamics of the renormalization operator. Then, we use the well-known Fenichel theory under rate conditions for normally hyperbolic invariant manifolds (we refer to [20]) to obtain a sharp estimate of the differentiability of Arnold tongues in terms of the spectrum of the linearized renormalization operator. Hence, we conclude that Arnold tongues are C^r , with r being a number such that

$$r \ge \frac{\log \delta}{\log \gamma}, \quad |\delta| > |\gamma| > 1,$$
 (1)

where δ is the leading unstable value of the linearization of a renormalization operator at the fixed point and γ is also another scaling factor related to renormalization (see the discussion in Sect. 5.2). In particular, these are "universal numbers" that do not depend on the family. We note that, even if the bounds are only lower bounds, there are reasons to believe that they are sharp and, as we will see this is consistent with our numerical findings.

We emphasize that, at the moment, we are presenting this renormalization group picture at the level of rigor of theoretical physics. A mathematically rigorous presentation would require significantly more details (such us specifying which Banach spaces of functions we are considering, domains of operators, etc.). We thing that it is more convenient to present an attractive picture that explains the rather delicate numerical observations presented in this paper. This picture is precise enough to lead to observable predictions.

The contents of the paper are organized as follows. In Sect. 2 we recall some fundamental facts about circle maps and Arnold tongues. Sect. 3 is devoted to describe the main numerical methods used in the paper. Some high-precision numerical computations are presented in Sect. 4 in order to give evidence of the differentiability of Arnold tongues. Then, the goal of Sect. 5 is to give some explanations of the observed phenomena in terms of the renormalization group. Finally, in Sect. 6, we present some additional numerical computations of Arnold tongues using the methods described in Sect. 3. Our findings are briefly summarized in Sect. 7.



2 Rotation Numbers and Arnold Tongues

In this section we briefly recall some basic definitions and concepts related to circle maps (for details see [17, 29]). We represent the circle as $\mathbb{T} = \mathbb{R}/\mathbb{Z}$ and define $\mathrm{Diff}_+^r(\mathbb{T})$, $r \in [0, +\infty) \cup \{\infty, \omega\}$, the group of orientation-preserving homeomorphisms of \mathbb{T} of class \mathcal{C}^r with inverse of class \mathcal{C}^r . Concretely, if r = 0, $\mathrm{Diff}_+^0(\mathbb{T})$ is the group of homeomorphisms of \mathbb{T} ; if $r \geq 1$, with $r \in (0, \infty) \setminus \mathbb{N}$, $\mathrm{Diff}_+^r(\mathbb{T})$ is the group of $\mathcal{C}^{[r]}$ -diffeomorphisms whose [r]th derivative verifies a Hölder condition with exponent r - [r]; if $r = \omega$, $\mathrm{Diff}_+^\omega(\mathbb{T})$ is the group of real analytic diffeomorphisms.

Given $f \in \operatorname{Diff}_+^r(\mathbb{T})$, we can lift f to \mathbb{R} by means of the universal cover $\pi : \mathbb{R} \to \mathbb{T}$, given by $\pi(x) = x \pmod{1}$, obtaining a C^r map \tilde{f} that makes the following diagram commute

$$\mathbb{R} \xrightarrow{\tilde{f}} \mathbb{R}$$

$$\pi \downarrow \qquad \qquad \downarrow_{\pi} \qquad \pi \circ \tilde{f} = f \circ \pi.$$

$$\mathbb{T} \xrightarrow{f} \mathbb{T}$$

Moreover, we have $\tilde{f}(x+1) - \tilde{f}(x) = 1$ (since f is orientation-preserving) and the lift is unique if we ask for $\tilde{f}(0) \in [0, 1)$. From now on, we choose the lift with this normalization so we can omit the tilde without any ambiguity and we can refer to *the* lift of a circle map.

Definition 2.1 Let f be the lift of an orientation-preserving homeomorphism of the circle. Then, the *rotation number of* f is defined as

$$\rho(f) := \pi \left(\lim_{|n| \to \infty} \frac{f^n(x_0) - x_0}{n} \right). \tag{2}$$

Let us recall some standard properties related to the rotation number (we refer to [29] for details). It is well known—already proved by Poincaré—that limit (2) exists for all $x_0 \in \mathbb{R}$ and is independent of x_0 . If we consider the rigid rotation $R_{\theta}(x) = x + \theta$, then $\rho(R_{\theta}) = \theta$. The rotation number ρ is continuous in the \mathcal{C}^0 -topology. If we consider the 1-parameter family $\mu \mapsto f_{\mu} = R_{\mu} \circ f$, with $f \in \text{Diff}^0_+(\mathbb{T})$, then $\theta(\mu) := \rho(f_{\mu})$ is an increasing function of μ and is strictly increasing when $\theta(\mu) \notin \mathbb{Q}$.

The rotation number is invariant under orientation-preserving conjugation, i.e., for every $f,h\in \mathrm{Diff}^0_+(\mathbb{T})$ we have that $\rho(h^{-1}\circ f\circ h)=\rho(f)$. Then, it is natural to investigate whether a particular circle map is conjugated to a rotation. A partial result was given by Denjoy (see [7]), ensuring that if $f\in \mathrm{Diff}^2_+(\mathbb{T})$ (actually, it suffices that the map has derivative of bounded variation) with $\rho(f)\in\mathbb{R}\setminus\mathbb{Q}$, then f is topologically conjugate to the rigid rotation $R_{\rho(f)}$, i.e., there exists $\eta\in\mathrm{Diff}^0_+(\mathbb{T})$ satisfying

$$f \circ \eta = \eta \circ R_{\rho(f)}. \tag{3}$$

In addition, if we require $\eta(0) = x_0$, for fixed x_0 , then the conjugacy η is unique. More interesting is to ask about the regularity of this conjugation. It is well-known that the answer depends on arithmetic properties of the rotation number.



Definition 2.2 Given $\theta \in \mathbb{R}$, we say that θ is a *Diophantine number* of (C, τ) type if there exist constants C > 0 and $\tau \ge 2$ such that for any $p/q \in \mathbb{Q}$

$$\left|\theta - \frac{p}{q}\right| > \frac{C}{|q|^{\tau}}.\tag{4}$$

We will denote $\mathcal{D}(C, \tau)$ the set of such numbers and \mathcal{D} the set of Diophantine numbers of any type.

The first result about smooth conjugation was given in [1], where is was proved that any analytic and close-to-rotation circle map f with Diophantine rotation number is analytically conjugate to $R_{\rho(f)}$. This result was extended in [24] to any map $f \in \text{Diff}_+^{\omega}(\mathbb{R})$. There have been subsequent improvements—the class of Diophantine numbers allowed, extensions to analytic maps, to lower differentiability, etc.

The following result is a particular case of the results in [58].

Theorem 2.3 If $f \in \text{Diff}_+^{\omega}(\mathbb{T})$ has rotation number in the class \mathcal{H} (which contains strictly the set of Diophantine numbers) then f is analytically conjugate to the rigid rotation $R_{\rho(f)}$.

Analogous results for $f \in \text{Diff}_+^r(\mathbb{R})$ where given in [30, 31, 50, 56]. As a sample, we mention the recent result [32], which provides the sharpest result in low regularity. These papers are particularly relevant for us, since they relate the conjugacy to properties of renormalization.

Theorem 2.4 If $f \in \operatorname{Diff}_+^r(\mathbb{T})$ has Diophantine rotation number $\rho(f) \in \mathcal{D}(C, \tau)$ for $2 \le \tau < r \le 3$ and $r - \tau < 1$, then f is $C^{1+r-\tau}$ -smoothly conjugate to the rigid rotation $R_{\rho(f)}$. In this result, r = 3 means that $f \in \operatorname{Diff}_+^{2+\operatorname{Lip}}(\mathbb{T})$.

The theory of smooth equivalence of critical circle maps has a less extensive literature. The interested reader is referred to [9, 10], which are based on renormalization ideas. In this paper we will consider the following class of critical maps.

Definition 2.5 The space of critical circle maps of order 2k + 1, that we denote as \mathfrak{C}^{2k+1} , is defined as the set of analytic functions f, that are strictly increasing in \mathbb{R} and satisfy

- f(x + 1) = f(x) + 1.
- $f^{(j)}(0) = 0$ for all $0 < j \le 2k$, and $f(0) f^{(2k+1)}(0) \ne 0$.
- There is no other critical point besides 0.

Now let us consider the following family of circle maps

$$f_{\omega,\varepsilon}^{A}(x) = x + \omega - \frac{\varepsilon}{2\pi} \sin(2\pi x),$$
 (5)

where $(\omega, \varepsilon) \in [0, 1) \times [0, 1]$ are parameters. Notice that this family satisfies $f_{\omega, \varepsilon}^A \in \mathrm{Diff}_+^\omega(\mathbb{T})$ for $\varepsilon < 1$ and $f_{\omega, 1}^A \in \mathfrak{C}^3$. Then, we obtain a function $(\omega, \varepsilon) \mapsto \rho(\omega, \varepsilon) := \rho(f_{\omega, \varepsilon}^A)$ given by the rotation number of the family (the map at the critical point is strictly increasing). Then, the *Arnold tongues* of (5) are defined as the sets

$$T_{\theta} = \{(\omega, \varepsilon) : \rho(\omega, \varepsilon) = \theta\},\$$



for any $\theta \in [0, 1)$.

It is well known that if $\theta \in \mathbb{Q}$, then generically, T_{θ} is a set with interior; otherwise, T_{θ} is a continuous curve which is the graph of a function $\varepsilon \mapsto \omega(\varepsilon)$, with $\omega(0) = \theta$. Furthermore, if $\theta \in \mathcal{D}$, the corresponding tongue is given by an analytic curve (see [38, 43]). To avoid confusions, we point out that the name Arnold tongue is sometimes used in the literature to refer only to the sets T_{θ} when $\theta \in \mathbb{Q}$.

For $\varepsilon = 1$ we have that $f_{\omega,1} \in \mathfrak{C}^3$ for every $\omega \in [0,1)$ —but is still an analytic map—and it is known (we refer to [16, 57]) that the conjugation to a rigid rotation is at most Hölder continuous. The main question that we face in this paper is if the function $\varepsilon \mapsto \omega(\varepsilon)$, for $\theta \in \mathcal{D}$, keeps some differentiability at $\varepsilon = 1$, something which is not predicted by KAM theory. We will study this problem using two different numerical methods. The numerical explanations will uncover several patterns. We will present a renormalization group explanation for them.

To illustrate several aspects of universality we select other families of circle maps in our computations (some interesting computations and properties of these families were reported in [16]), namely the *cubic critical family*

$$f_{\omega,\varepsilon}^{C}(x) = x + \omega - \frac{\varepsilon}{2\pi} \left(\kappa \sin(2\pi x) + \frac{1 - \kappa}{2} \sin(4\pi x) \right), \tag{6}$$

and the quintic critical family

$$f_{\omega,\varepsilon}^{\mathcal{Q}}(x) = x + \omega - \frac{\varepsilon}{2\pi} \left(\kappa \sin(2\pi x) + \frac{9 - 8\kappa}{10} \sin(4\pi x) + \frac{3\kappa - 4}{15} \sin(6\pi x) \right). \tag{7}$$

Both families satisfy that $f_{\omega,\varepsilon}^C$, $f_{\omega,\varepsilon}^Q \in \mathrm{Diff}_+^\omega(\mathbb{T})$ for $\varepsilon < 1$. Furthermore, for $\varepsilon = 1$ we have that $f_{\omega,\varepsilon}^C \in \mathfrak{C}^3$ for $0 \le \kappa < \frac{4}{3}$ and $f_{\omega,\varepsilon}^C \in \mathfrak{C}^5$ for $\kappa = \frac{4}{3}$. Analogously, for $\varepsilon = 1$ we have that $f_{\omega,\varepsilon}^Q \in \mathfrak{C}^5$ for $\frac{1}{2} \le \kappa < \frac{3}{2}$ and $f_{\omega,\varepsilon}^C \in \mathfrak{C}^7$ for $\kappa = \frac{3}{2}$.

Finally, let us observe that the families (5), (6) and (7) are non-generic in the sense that their maps contain a finite number of harmonics. For this reason, we consider also the Arnold family with infinite harmonics

$$f_{\omega,\varepsilon}^{H}(x) = x + \omega - \frac{\varepsilon}{2\pi} \frac{(1 - \kappa)\sin(2\pi x)}{1 - \kappa\cos(2\pi x)},\tag{8}$$

for $0 < \kappa < 1$.

3 Numerical Methods

In this section we describe the two main numerical methods that we use in the present paper. Firstly, in Sect. 3.1 we include a brief survey of methods developed in [35, 46] to compute rotation numbers of circle maps and derivatives with respect to parameters. Secondly, in Sect. 3.2 we introduce a method (adapting ideas presented in [2, 14, 37, 38, 59, 60]) to compute numerically Arnold tongues together with a very accurate approximation of the conjugacy at every point. Both methods are very efficient and fast, as we summarize next:

• If we compute N iterates of the map, then the averaging-extrapolation method supported by Proposition 3.1 allows us to approximate the rotation number with an error of order $\mathcal{O}(1/N^{p+1})$ where p is the selected order of averaging (compared with $\mathcal{O}(1/N)$ obtained



using the definition). Similarly, we can approximate derivatives of order d with an error of order $\mathcal{O}(1/N^{p+1-d})$. Algorithm 3.2, corresponding to this procedure, requires $\mathcal{O}(Np) = \mathcal{O}(N\log_2 N)$ operations (see Remark 3.4).

• If we use N Fourier coefficients, then the method in Sect. 3.2 allows to approximate the conjugacy of the circle map to a rigid rotation with an exponentially small error. The idea is to perform a Newton method where every correction consists of a small number of steps, each of which is diagonal either in real space or in Fourier space. Fast Fourier Transform allows passing from real space to Fourier space so the cost of one step of the Newton method is of $\mathcal{O}(N\log_2 N)$ operations and $\mathcal{O}(N)$ in memory. Implementation is described in Algorithm 3.5.

3.1 An Extrapolation Method to Compute Rotation Numbers and Its Derivatives with Respect to Parameters

For the sake of completeness, we review here the method developed in [46] for computing Diophantine rotation numbers of analytic circle diffeomorphisms (the C^r case is similar) that was later extended in [35] to compute derivatives with respect to parameters.

Let us consider $f \in \mathrm{Diff}_+^\omega(\mathbb{T})$ with rotation number $\theta = \rho(f) \in \mathcal{D}$. Notice that we can write the conjugacy of Theorem 2.3 as $\eta(x) = x + \xi(x)$, ξ being a 1-periodic function normalized in such a way that $\xi(0) = x_0$, for a fixed $x_0 \in [0, 1)$. Now, by using the fact that η conjugates f to a rigid rotation, we can write the iterates under the lift as follows

$$f^{n}(x_{0}) = f^{n}(\eta(0)) = \eta(n\theta) = n\theta + \sum_{k \in \mathbb{Z}} \hat{\xi}_{k} e^{2\pi i k n\theta}, \quad \forall n \in \mathbb{Z},$$
(9)

where the sequence $\{\hat{\xi}_k\}_{k\in\mathbb{Z}}$ denotes the Fourier coefficients of ξ . Then, we have

$$\frac{f^{n}(x_{0}) - x_{0}}{n} = \theta + \frac{1}{n} \sum_{k \in \mathbb{Z}_{*}} \hat{\xi}_{k} (e^{2\pi i k n \theta} - 1),$$

that allows computing θ modulo terms of order $\mathcal{O}(1/n)$. The idea of [46] is to average the iterates $f^n(x_0)$ in a suitable way, obtaining a smaller quasi-periodic remainder.

As a motivation, let us start by considering the sum of the first N iterates under f (expressed as in (9))

$$S_N^1(f) := \sum_{n=1}^N (f^n(x_0) - x_0) = \frac{N(N+1)}{2}\theta - N\sum_{k \in \mathbb{Z}_*} \hat{\xi}_k + \sum_{k \in \mathbb{Z}_*} \hat{\xi}_k \frac{e^{2\pi i k\theta} (1 - e^{2\pi i kN\theta})}{1 - e^{2\pi i k\theta}}.$$
 (10)

We observe that the factor multiplying θ in (10) grows quadratically with the number of iterates, while the next term is linear in N, with constant $A_1 = -\sum_{k \in \mathbb{Z}_*} \hat{\xi}_k$. Moreover, the quasi-periodic sum remains uniformly bounded since, by hypothesis, θ is Diophantine and η is analytic. Thus, we obtain

$$\frac{2}{N(N+1)}S_N^1(f) = \theta + \frac{2}{N+1}A_1 + \mathcal{O}(1/N^2),\tag{11}$$

that allows us to extrapolate the value of θ with an error $\mathcal{O}(1/N^2)$ if, for example, we compute $S_N^1(f)$ and $S_{2N}^1(f)$. Higher order extrapolation follows in a similar way (see Algorithm 3.1). We refer to [46] for the precise formulas and the combinatorial details.



Besides the rotation number, we are interested in computing derivatives with respect to parameters. Let us consider a family $\mu \in I \subset \mathbb{R} \mapsto f_{\mu} \in \mathrm{Diff}^{\omega}_{+}(\mathbb{T})$ depending \mathcal{C}^{d} -smoothly with respect to μ . The corresponding rotation numbers induce a function $\theta: I \to [0,1)$ given by $\theta(\mu) = \rho(f_{\mu})$. It is well-known that the function θ is continuous but non-smooth: generically, there exist a family of disjoint open intervals of I, with dense union, such that θ takes distinct constant values on these intervals (a so-called Devil's Staircase, see for example [29]). However, the derivatives of θ are defined in "many" points in the sense of Whitney.

Concretely, let $J \subset I$ be the subset of parameters such that $\theta(\mu) \in \mathcal{D}$ (typically a Cantor set). Then, from Theorem 2.3, there exists a family of conjugacies $\mu \in J \mapsto \eta_{\mu} \in \mathrm{Diff}_{+}^{\omega}(\mathbb{T})$, satisfying $f_{\mu} \circ \eta_{\mu} = \eta_{\mu} \circ R_{\theta(\mu)}$, that is unique if we fix $\eta_{\mu}(0) = x_0$. Then, if f_{μ} is \mathcal{C}^s with respect to μ , the Whitney derivatives $D^j_{\mu}\eta_{\mu}$ and $D^j_{\mu}\theta$, for $j=1,\ldots,s$, can be computed by taking formal derivatives with respect to μ on the conjugacy equation and solving small divisors equations thus obtained. Actually, we know that, if we define $J(C,\tau)$ as the subset of J such that $\theta(\mu) \in \mathcal{D}(C,\tau)$, then the maps $\mu \in J(C,\tau) \mapsto \eta_{\mu}$ and $\mu \in J(C,\tau) \mapsto \theta$ can be extended to \mathcal{C}^d functions on I, where $d = d(s,\tau)$, provided that d is big enough (see [53]).

To compute $D_{\mu}^{d}\theta(\mu_{0})$, the *d*-th derivative with respect to μ at μ_{0} , with $d \geq 0$ —let us remark that we are including formally the case $D_{\mu}^{0}\theta(\mu_{0}) = \theta(\mu_{0})$ —, we introduce *recursive* sums of order p (we omit the notation regarding the fact that the map is evaluated at $\mu = \mu_{0}$)

$$D_{\mu}^{d}S_{N}^{0} = D_{\mu}^{d}(f_{\mu}^{N}(x_{0}) - x_{0}), \qquad D_{\mu}^{d}S_{N}^{p} = \sum_{j=0}^{N} D_{\mu}^{d}S_{j}^{p-1},$$

and the corresponding averaged sums

$$D^d_{\mu}\tilde{S}^p_N = \binom{N+p}{p+1}^{-1} D^d_{\mu} S^p_N.$$

Then, the following result holds (we refer to [46] for d = 0 and [35] for d > 0) by induction and using the regularity properties of the conjugacy in Theorem 2.3.

Proposition 3.1 If $\theta(\mu_0) \in \mathcal{D}$ and the derivatives $D^j_{\mu}\theta(\mu_0)$ for j = 0, ..., d exist, then the following expression holds

$$D_{\mu}^{d}\tilde{S}_{N}^{p} = D_{\mu}^{d}\theta + \sum_{l=1}^{p-d} \frac{D_{\mu}^{d}A_{l}^{p}}{N^{l}} + D_{\mu}^{d}E^{p}(N), \tag{12}$$

where the coefficients $D^d_\mu A^p_l$ are independent of N and the remainder $D^d_\mu E^p(N)$ is of order $\mathcal{O}(1/N^{p-d+1})$.

Therefore, according to formula (12), we implement the following algorithm to extrapolate the d-th derivative of the rotation number.

Algorithm 3.2 Once an averaging order p is selected, we take $N=2^q$ iterates of the map, for some q>p, and compute the sums $\{D_{\mu}^d \tilde{S}_{N_j}^p\}_{j=0,\dots,p-d}$ with $N_j=2^{q-p+j+d}$. We approximate the d-th derivative of the rotation number (including the case d=0) using the



formula

$$D_{\mu}^{d}\theta = \Theta_{q,p,p-d}^{d} + \mathcal{O}(2^{-(p-d+1)q}), \qquad \Theta_{q,p,m}^{d} = \sum_{j=0}^{m} c_{j}^{(m)} D_{\mu}^{d} \tilde{S}_{2^{q-m+j}}^{p},$$

where the coefficients $c_i^{(m)}$ are given by

$$c_l^{(m)} = (-1)^{m-l} \frac{2^{l(l+1)/2}}{\delta(l)\delta(m-l)},\tag{13}$$

with $\delta(n) := (2^n - 1)(2^{n-1} - 1) \cdots (2^1 - 1)$ for $n \ge 1$ and $\delta(0) := 1$. The operator $\Theta_{q,p,p-d}^d$ corresponds to the Richardson extrapolation of order p - d of (12).

Remark 3.3 To approximate derivatives of the rotation number, we require to compute efficiently the quantities $D_{\mu}^{d}(f_{\mu}^{n}(x))$, i.e., the derivatives with respect to the parameter of the iterates of an orbit. To this end, algorithms based on recursive and combinatorial formulas are detailed in [35].

Remark 3.4 Given an averaging order p and a number of iterates $N=2^q$, the cost of computing $\{D_{\mu}^d \tilde{S}_{N_j}^p\}_{j=0,\dots,p-d}$ is of order $\mathcal{O}(2^q p)$. Taking into account that (given a value of q) the optimal value of p to use in the extrapolation is $p \simeq q - (\tau + 1) \log_2(q)$ —see details in [46]—we obtain that the computational cost of Algorithm 3.2 is $\mathcal{O}(2^q p) = \mathcal{O}(N \log_2 N)$. Furthermore, let us remark that the implementation of this algorithm does not require to store any intermediate value, so it has negligible memory cost.

In this case, we obtain the following heuristic expression for the extrapolation error (more details are given in [46])

$$|D_{\mu}^{d}\theta - \Theta_{q,p,p-d}^{d}| \le \frac{10}{2^{p-d+1}} |\Theta_{q,p,p-d}^{d} - \Theta_{q-1,p,p-d}^{d}|. \tag{14}$$

Notice that if we select an averaging order p, then we are limited to extrapolate with order p-d. Moreover, p is the maximum order of the derivative that can be computed.

3.2 A Fast Newton Method for Computing Arnold Tongues

Another numerical approach to compute Arnold tongues T_{θ} , with $\theta \in \mathcal{D}$, is based in a posteriori methods introduced in [37, 38]. This has the advantage that it allows obtaining at the same time an approximation of the conjugacy to a rigid rotation and its Fourier coefficients. Let us assume that (for certain ε which is not explicitly mentioned) the conjugacy relation in (3) is satisfied with certain error, i.e., given $f_{\omega} \in \mathrm{Diff}^{\omega}_{+}(\mathbb{T})$ and θ we have an approximate conjugacy h such that

$$f_{\omega}(h(x)) = h(x+\theta) + e(x), \tag{15}$$

where $e: \mathbb{T} \to \mathbb{T}$ is an error function. To implement a Newton method, we consider corrections $\bar{\omega} = \omega + \Delta_{\omega}$ and $\bar{h} = h + \Delta_h$ which are obtained by solving (at least approximately) the following linearized equation

$$f'_{\omega}(h(x))\Delta_h(x) - \Delta_h(x+\theta) + \partial_{\omega}f_{\omega}(h(x))\Delta_{\omega} = -e(x).$$



Following [37, 38] we write

$$\Delta_h(x) = h'(x)\varphi(x),$$

thus obtaining

$$f'_{\omega}(h(x))h'(x)\varphi(x) - h'(x+\theta)\varphi(x+\theta) + \partial_{\omega}f_{\omega}(h(x))\Delta_{\omega} = -e(x).$$
 (16)

Notice that taking derivatives at both sides of (15) we get

$$f'_{\omega}(h(x))h'(x) = h'(x+\theta) + e'(x),$$

and introducing this expression into (16), we obtain (using that $h'(x + \theta) \neq 0$)

$$\varphi(x) - \varphi(x + \theta) = v(x), \quad v(x) := -\frac{\partial_{\omega} f_{\omega}(h(x))\Delta_{\omega} + e(x)}{h'(x + \theta)}$$
(17)

modulo quadratic terms in the error. Solutions of cohomological equation (17) are easy to find using Fourier series for periodic functions

$$f(x) = \sum_{k \in \mathbb{Z}} \hat{f}_k e^{2\pi i kx},$$

where we denote $[f]_{\mathbb{T}} = \hat{f}_0$ the average of f. Thus, we obtain that—the correction in Δ_{ω} is obtained from the compatibility condition $[v]_{\mathbb{T}} = 0$ —

$$\Delta_{\omega} = -\frac{[e]_{\mathbb{T}}}{[\partial_{\omega} f_{\omega} \circ h]_{\mathbb{T}}}, \qquad \hat{\varphi}_{k} = \frac{\hat{v}_{k}}{1 - e^{2\pi i k \theta}}, \qquad k \in \mathbb{Z} \setminus \{0\},$$
(18)

the solution being unique if we fix the average $[\varphi]_{\mathbb{T}}$. Cohomological equation as (17) are standard in KAM theory (see for instance [12, 44]) and it is well-known that under Diophantine conditions given by (4) we can control the analyticity of φ —optimal estimates where provided in [44]—and the convergence of the obtained quadratic scheme. The reader interested in convergence proofs is referred to [1, 12, 37, 38, 59, 60].

Following the above scheme, we can implement an efficient algorithm to perform a quasi-Newton step in the computation of the Arnold tongue. The main idea is to take advantage of the fact that solutions of cohomological equations obtained in (18)—and also the computation of derivatives such as h'—are diagonal operators in Fourier space. At the same time, other algebraic operations of functions (product, addition, quotient) as well as compositions can be performed efficiently in real space and there are very fast and robust FFT algorithms that allows passing from real to Fourier space (and "vice versa"). Accordingly, if we approximate the periodic functions involved by using N Fourier modes, we can implement an algorithm to compute the object with a cost of order $\mathcal{O}(N\log_2 N)$ in time and $\mathcal{O}(N)$ in memory. We refer to [2, 14, 28] for related algorithms in several contexts.

All computations presented in this paper have been performed using truncated Fourier series up to order $N=2^q$, with $q\in\mathbb{N}$, corresponding to the discrete Fourier transform associated to N equispaced points in real space $\{f_j\}=\{f_j\}_{j=0,\dots,N-1}$, with $f_j=f(j/N)$. In the following discussion, we will denote

$$\{\hat{f}_k\} = \text{FFT}_N(\{f_j\}), \quad \text{with } \hat{f}_k = \frac{1}{N} \sum_{i=0}^{N-1} f_j e^{-2\pi i k j/N},$$
 (19)

where $\hat{f}_0 \in \mathbb{R}$, $\hat{f}_k = \hat{f}_{N-k}^*$ and, for convenience, we set $\hat{f}_{N/2} = 0$. Conversely we denote $\{f_i\} = \text{FFT}_N^{-1}(\{\hat{f}_k\})$.

Algorithm 3.5 One step of Newton method Given a circle map $f_{\omega} \in \operatorname{Diff}_{+}^{\omega}(\mathbb{T})$ and a rotation number θ , let us assume that we have an approximate conjugacy $h(x) = x + \xi(x)$ to a rigid rotation R_{θ} , which is given by N Fourier coefficients $\{\hat{\xi}_k\}$ (see Remark (19)). Then, we perform the following computations:

- 1. Estimation of the error.
 - (a) Compute $\{\xi_i\} = \text{FFT}_N^{-1}(\{\hat{\xi}_k\})$.
 - (b) Compute the Fourier coefficients of $\xi^{\theta} = \xi \circ R_{\theta}$ using $\hat{\xi}_{k}^{\theta} = \hat{\xi}_{k} e^{2\pi i \theta}$.
 - (c) Compute $\{\xi_i^{\theta}\} = \text{FFT}_N^{-1}(\{\hat{\xi}_k^{\theta}\}).$
 - (d) Compute $\{h_j^i\}$ and $\{h_j^\theta\}$ using $h_j = j/N + \xi_j$ and $h_j^\theta = \theta + j/N + \xi_j^\theta$.
 - (e) Compute $\{e_j\}$ using $e_j = f_{\omega}(h_j) h_j^{\theta}$.
- 2. Solution of the cohomological equation.
 - (a) Compute the Fourier coefficients of ξ' using $\hat{\xi}'_k = 2\pi i k \hat{\xi}_k$.
 - (b) Compute the Fourier coefficients of $\hat{\xi}'^{\theta}$ using $\hat{\xi}_{k}^{'\theta} = \hat{\xi}_{k}' e^{2\pi i \theta}$.
 - (c) Compute $\{\xi_i^{\prime\theta}\} = \text{FFT}_N^{-1}(\{\hat{\xi}_k^{\prime\theta}\}).$
 - (d) Compute $\{a_i\}$ and $\{b_i\}$ by means of

$$a_j = -e_j/(1 + \xi_j^{\theta})$$
 and $b_j = -\partial_{\omega} f_{\omega}(h_j)/(1 + \xi_j^{\theta})$.

- (e) Compute $\{\hat{a}_k\} = \text{FFT}_N(\{a_i\})$ and $\{\hat{b}_k\} = \text{FFT}_N(\{b_i\})$.
- (f) Compute $\Delta_{\omega} = -a_0/b_0$.
- (g) Compute $\{\hat{v}_k\}$ using $\hat{v}_k = \hat{a}_k + \hat{b}_k \Delta_{\omega}$.
- (h) Compute $\{\hat{\varphi}_k\}$ using $\hat{\varphi}_k = \hat{v}_k/(1 e^{2\pi i k\theta})$ and $\{\varphi_j\} = FFT_N^{-1}(\{\hat{\varphi}_k\})$.
- 3. Correction of the conjugacy.
 - (a) Compute $\{\xi_{j}'\} = FFT_{N}^{-1}(\{\hat{\xi}_{k}'\})$.
 - (b) Compute the new approximately conjugacy $\{\xi_j\}$ using $\xi_j \leftarrow \xi_j + (1 + \xi_j')\varphi_j$.
 - (c) Compute $\{\hat{\xi}_k\} = \text{FFT}_N(\{\xi_i\})$.

Remark 3.6 Consider the *r*-Sobolev norm given by

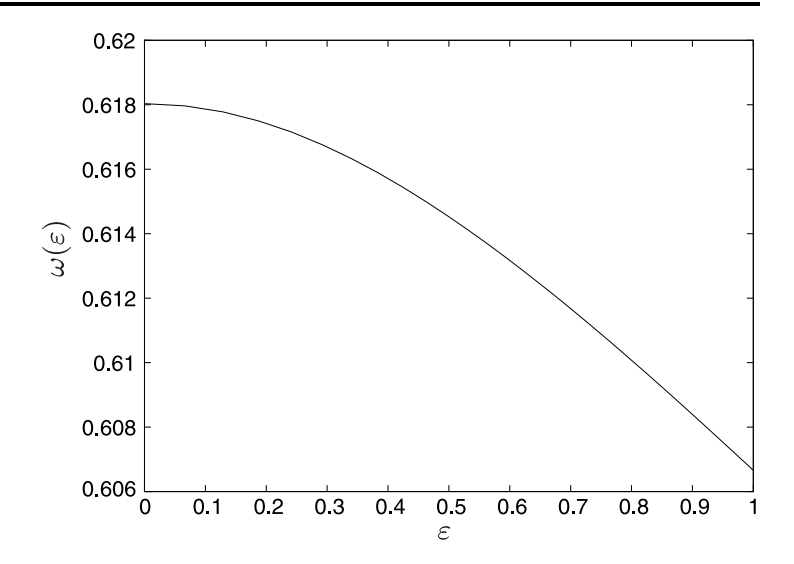
$$||f||_{H^r} = ||D^r f||_{L^2} = \left(\sum_{k \ge 0} (2\pi k)^{2r} |\hat{f}_k|^2\right)^{\frac{1}{2}}.$$
 (20)

Then, we observe that Algorithm 3.5 allows us to monitor the evolution of these norms along Arnold tongues. Therefore, we can study the breakdown of regularity of the conjugacy when approaching the critical point (see computations in Sect. 6).

Remark 3.7 To apply Algorithm 3.5, we recall that the conjugacy corresponding to the point $(\omega, \varepsilon) = (\theta, 0)$ is given by $\{\hat{\xi}_k\} = 0$. We start the computations using $N_0 = 2^8$ Fourier coefficients and we control the number of coefficients at the *i*th step by studying the size of the last N/2 coefficients in $\{\xi_k\}$. Notice also that truncation to finite dimension may produce spurious solutions and one possibility to avoid this spurious solutions is by using adaptive steps in the Newton method. We refer to [2] for details.



Fig. 1 Graph of $\varepsilon \mapsto \omega(\varepsilon)$ corresponding to the Arnold tongue T_{θ} , for the fixed rotation number $\theta = (\sqrt{5} - 1)/2$



4 First Numerical Explorations

Using the approach described in Sect. 3.1, some Arnold tongues T_{θ} of Diophantine rotation number were approximated in [46] using the secant method and in [35] using the Newton method. To do that, one fixes $\theta \in \mathcal{D}$ and solves the equation $\rho(\omega, \varepsilon) - \theta = 0$ by continuing the known solution $(\theta, 0)$ with respect to ε (we refer to these references for details). Here we are interested in the continuation of such solutions when ε approaches the critical value, $\varepsilon = 1$. We have found empirically that, when approaching the critical point, it is better to use the secant method to avoid the phase-locking regions.

As implementation parameters we take an averaging order p = 9 and $N = 2^q$ iterates of the map, with $q \le 23$. Computations have been performed using a GNU C++ compiler and the multiple arithmetic has been provided by the routines *quad-double package* of [26], which include a *quadruple-double* data type of approximately 64 digits.

First we compute the Arnold tongue T_{θ} , with $\theta = \frac{\sqrt{5}-1}{2}$, corresponding to family (5). The continuation step in ε is taken as 0.01 if $\varepsilon \le 0.99$. Beyond this value, we consider the points $\varepsilon = 1 - 0.95^{n/10}$, for 1000, 1001, ..., 2010. Notice that the selected points approach exponentially fast to the critical point and they are defined using the fraction n/10 just following a criterion of parallelization.

In Fig. 1 we plot the graph of this Arnold Tongue, and in the left plot of Fig. 2 we show, in \log_{10} - \log_{10} scale, the derivatives of the rotation number with respect to ω and ε along the computed tongue.

Fitting these computations we obtain the following asymptotic expressions close to the critical point (for $\varepsilon \simeq 1$)

$$D_{\omega}\rho(\omega(\varepsilon),\varepsilon) \simeq \frac{0.884...}{(1-\varepsilon)^{0.155...}}, \qquad D_{\varepsilon}\rho(\omega(\varepsilon),\varepsilon) \simeq \frac{0.015...}{(1-\varepsilon)^{0.155...}}.$$
 (21)

In the right plot of Fig. 2 we show the estimated extrapolation error by means of formula (14). We note that asymptotic expansions (21) are modulated by a log-periodic factor. This is a prediction of the renormalization group picture. Indeed, the renormalization group picture predicts that if we scale the parameters by a factor δ , the regularity features scale by another factor. This scaling relations are satisfied by power laws multiplied by a log-periodic function of log-period δ . These log-period corrections were an important tool in [16].



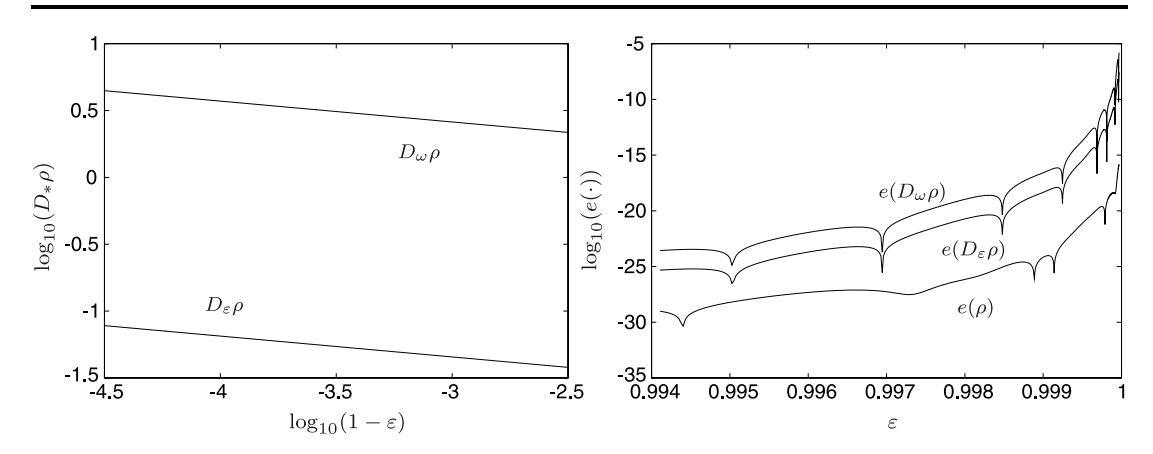


Fig. 2 Left: Graph of the derivatives $\log_{10}(1-\varepsilon) \mapsto \log_{10} D_{\omega} \rho(\omega(\varepsilon), \varepsilon)$ (upper graph) and $\log_{10}(1-\varepsilon) \mapsto \log_{10} D_{\varepsilon} \rho(\omega(\varepsilon), \varepsilon)$ (lower graph) along T_{θ} , for the fixed rotation number $\theta = (\sqrt{5} - 1)/2$. Right: We plot $\varepsilon \mapsto \log_{10}(e(\cdot))$, where $e(\cdot)$ stands for the heuristically estimated error—see (14)—in the computation of the rotation number and its derivatives

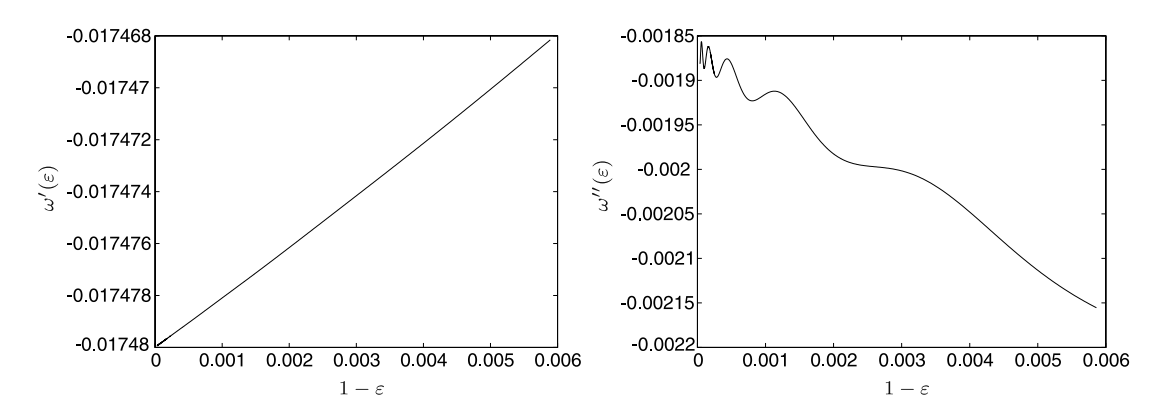


Fig. 3 Left: Graph of the derivative $(1 - \varepsilon) \mapsto \omega'(\varepsilon)$ along T_{θ} , with $\theta = (\sqrt{5} - 1)/2$, computed as (22) from the data in the left plot of Fig. 2. Right: Graph of the derivative $(1 - \varepsilon) \mapsto \omega''(\varepsilon)$ along T_{θ} , with $\theta = (\sqrt{5} - 1)/2$, computed as (23)

For ε < 0.99, the errors in the computations are of the order of the precision of the machine. When we are far from the critical point—by "far" we mean a distance larger than 0.001—we can compute the rotation number with more than 25 digits, and the precision of our computations decreases when approaching the critical point.

The observed growth of the derivatives given in (21) suggests that the map $\varepsilon \mapsto \omega(\varepsilon)$ is \mathcal{C}^1 at $\varepsilon = 1$ —in the left plot of Fig. 3 we show the derivative of this map close to the critical point—since

$$\omega'(\varepsilon) = -\frac{D_{\varepsilon}\rho(\omega(\varepsilon), \varepsilon)}{D_{\omega}\rho(\omega(\varepsilon), \varepsilon)}.$$
(22)

Generalization of formula (22) to higher order is straightforward. However, the growth of higher order derivatives of the rotation number does not allow us to assert straightforwardly the existence of derivatives of higher order of $\omega(\varepsilon)$ at $\varepsilon = 1$. For example, the second derivative is given by

$$\omega''(\varepsilon) = \frac{-(D_{\omega\omega}\rho(\omega(\varepsilon), \varepsilon)\omega'(\varepsilon) + 2D_{\omega\varepsilon}\rho(\omega(\varepsilon), \varepsilon))\omega'(\varepsilon) - D_{\varepsilon\varepsilon}\rho(\omega(\varepsilon), \varepsilon)}{D_{\omega}\rho(\omega(\varepsilon), \varepsilon)}.$$
 (23)



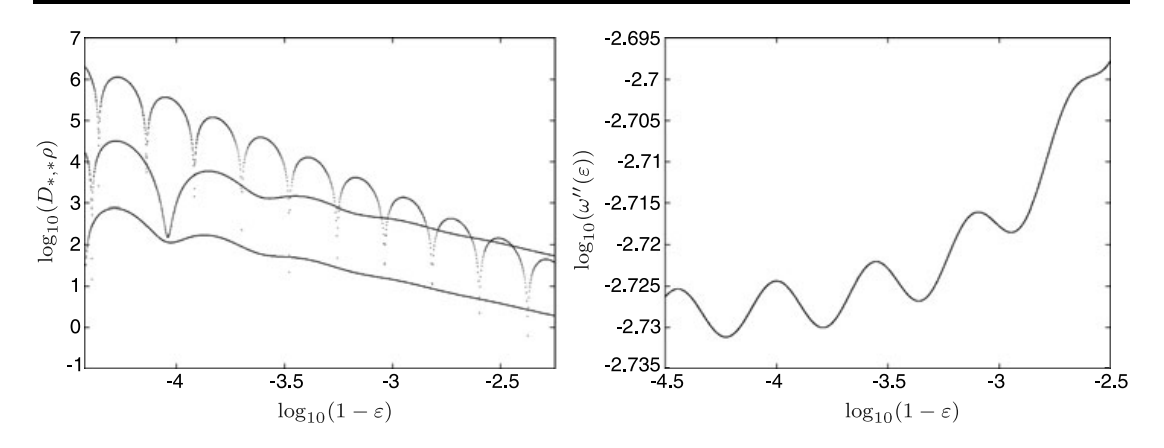


Fig. 4 Left: Graph in \log_{10} - \log_{10} scale of the derivatives $D_{\omega,\omega}\rho(\omega(\varepsilon),\varepsilon)$ (upper graph), $D_{\omega,\varepsilon}\rho(\omega(\varepsilon),\varepsilon)$ (middle graph) and $D_{\varepsilon,\varepsilon}\rho(\omega(\varepsilon),\varepsilon)$ (lower graph) along T_{θ} . These derivatives satisfy an expression like (21) (modulo periodic corrections) with an exponent 2.16435 rather than 0.15604. Right: Graph of the derivative $\log_{10}(1-\varepsilon)\mapsto\log_{10}(\omega''(\varepsilon))$ along T_{θ} , with $\theta=(\sqrt{5}-1)/2$, computed as (23)

From our numerical experiments we observe that the second order derivatives $D_{\omega\omega}\rho$, $D_{\omega\varepsilon}\rho$ and $D_{\varepsilon\varepsilon}\rho$ grow much faster than $D_{\omega}\rho$ (see the left plot of Fig. 4), so a necessary condition to ensure that $\omega''(\varepsilon)$ exists is that some precise cancellations take place in the numerator. Indeed, our numerical experiments indicate that $\omega''(\varepsilon)$ is bounded (see the right plot of Fig. 3) so that significant cancellations among terms in the numerator in (23) are taking place. In other words, the numerator is much smaller than each of the individual terms forming it. We think that these rather striking cancellations among terms that look so different is an evidence in favor of the existence of a renormalization picture and that the features at breakdown are driven by scaling arguments.

Moreover, we see in Fig. 4 that there are oscillations that seem almost log-periodic (they decay exponentially, albeit very slowly). We can therefore expect that the Arnold tongue has a regularity slightly bigger than \mathcal{C}^2 . As we will see, the renormalization group picture to be discussed in Sect. 5.2 predicts that this curve is $\mathcal{C}^{2+0.05}$.

Remark 4.1 We notice that the extrapolation error in the computation of second order derivatives increases dramatically when approaching $\varepsilon = 1$, and one may thing that the oscillations observed correspond to this error. However, due to the accuracy of the computations shown in the left plot of Fig. 3, we can approximate $\omega''(\varepsilon)$ using finite differences thus obtaining the same graph shown in the right plot of Fig. 3.

Remark 4.2 A similar behavior is observed for other rotation numbers (see Sect. 6). In all the cases, the curves are shown to be smoother than C^1 . The curve corresponding to the golden mean is the only one (among the computed rotation numbers) that is smoother than C^2 .

5 Explanations in Terms of Renormalization Group

Numerical computations described in Sect. 4 suggest that Diophantine Arnold tongues maintain some differentiability at the critical point (outside the domain of applicability of KAM theory), even though these sets correspond to level curves of a function—the rotation number—whose derivatives blow-up at the critical point.

Our goal now is to justify the differentiability observed. In particular, in Sect. 5.1 we use the properties of cumulant operators to characterize the growth of the first derivatives



of the rotation number with respect to parameters. We will see that the asymptotic behavior of these derivatives is the same. Then, in Sect. 5.2 we give an explanation of the borderline regularity based on a renormalization group picture. Then, we use the well-known Fenichel theory under rate conditions for normally hyperbolic invariant manifolds to give a sharp estimate of the differentiability of Arnold tongues. This depends on the spectrum of the linearized renormalization operator and it is at least $\mathcal{C}^{1+\alpha}$.

We emphasize again that we present the results at the level of precision common in theoretical physics and not at the level of complete mathematical rigor. Notably, we will talk about eigenvalues of the linearization without specifying on which spaces the functions act on. There are mathematical reasons as well as experience showing that the points of the spectrum which matter for our argument are largely independent of what are the spaces considered.

5.1 Renormalization Group and Cumulant Operators Formalism

In this section we recall some basic ideas, regarding renormalization group theory, required to understand results reported in [5, 6], where the effect of dynamical noise in one-dimensional critical dynamical systems (namely unimodal maps of the interval at the accumulation of period-doubling and critical circle maps) is studied. In these references, a renormalization scheme was developed for the system

$$x_n = f(x_{n-1}) + \sigma \xi_n \tag{24}$$

where f is either a unimodal or a critical circle map, ξ_n are zero mean independent random variables, and $\sigma \ge 0$ is a small parameter which measures the size of the bare noise. The goal was to obtain some scaling relations for the Wick ordered moments (called "cumulants" by statisticians) of the effective noise, and to show that there is a well defined scaling limit.

It turns out that the same asymptotic properties of cumulant operators characterize the growth of the different derivatives of the rotation number (see Proposition 5.1), which is the interest of this paper. The goal of this section is to use the scaling properties obtained for these derivatives to obtain the following result.

Proposition 5.1 Let us consider a two parametric family $(\omega, \varepsilon) \mapsto f_{\omega,\varepsilon}$ of analytic circle diffeomorphisms, such that for $\varepsilon = 1$ we have that $f_{\omega,1} \in \mathfrak{C}^{2k+1}$. Let us consider the Arnold tongue T_{θ} of rotation number $\theta = \frac{\sqrt{5}-1}{2}$. Then, under certain hypothesis on the renormalization group (see the discussion below), we have that the quotient

$$\frac{D_{\varepsilon}[f_{\omega,\varepsilon}^n](x)}{D_{\omega}[f_{\omega,\varepsilon}^n](x)}$$

is uniformly bounded with respect to n, for every (ω, ε) in the closure of T_{θ} .

For the purposes of this section, we will resort only to some basic properties of the scaling limits of renormalized maps that we summarize next (we follow [33]). From the well-known relation between the golden mean and the Fibonacci sequence $\{F_n\}_{n\in\mathbb{Z}}$, given by $F_0 = 0$, $F_1 = 1$ and $F_{n+1} = F_n + F_{n-1}$, it follows that

$$\theta = \lim_{n \to \infty} \frac{F_n}{F_{n+1}}, \qquad F_n \theta - F_{n-1} = (-1)^{n-1} \theta^n,$$



and also that the rotation number of

$$f_{(n)}(x) = f^{F_n}(x) - F_{n-1}$$

equals $(-1)^{n-1}\theta^n$. Notice that for n large $\rho(f_{(n)})$ is small, so we have that $f_{(n)}(x) \simeq x$ as $x \simeq 0$. We want to concentrate on the behavior of $f_{(n)}$ near the critical point (recall that f'(0) = 0) and we therefore magnify as follows: let us introduce $\alpha_{(n)} = f_{(n)}(0)^{-1}$ and the n-1th renormalization of f

$$\mathcal{R}_{n-1}[f](x) := f_n(x) = \alpha_{(n-1)} f_{(n)}(x/\alpha_{(n-1)}). \tag{25}$$

Remark 5.2 Since $\rho(f_{(n)}) = (-1)^{n-1}\theta^n$, we have that

$$(-1)^{n-1}(f_{(n)}(x)-x)>0$$

for all $n \in \mathbb{N}$ and $x \in \mathbb{R}$. In particular, for x = 0 we obtain that $(-1)^{n-1}\alpha_{(n)} > 0$. Therefore it follows that each function $f_n(x)$ is increasing in x and satisfies $f_n(x) < x$.

Numerical experiments (see the references given in Sect. 1) suggest that for every $k \in \mathbb{N}$ there is a universal constant α_* , satisfying $\alpha_* < -1$, and a universal function f_* , both depending on k, such that

- (1) The sequence of ratios $\alpha_n = \alpha_{(n+1)}/\alpha_{(n)}$ converges to α_* .
- (2) The sequence of functions f_n converges to f_* (non-trivial fixed point).

Then, let us observe that $f_n(0) = \alpha_{(n-1)} f_{(n)}(0) = \alpha_n^{-1}$, and we obtain

$$\alpha_* = \lim_{n \to \infty} f_n(0)^{-1} = f_*(0)^{-1}$$
(26)

(for example, for the cubic case k=1 we have $\alpha_* \simeq -1.2885745...$). Moreover, using that $F_{n+1} = F_n + F_{n-1}$, it follows that $f_{(n+1)} = f_{(n)} \circ f_{(n-1)}$ and also $f_{(n+1)} = f_{(n-1)} \circ f_{(n)}$. After a suitable rescaling by $\alpha_{(n)}$, from these expressions we obtain, respectively,

$$f_{n+1}(x) = \alpha_n f_n(\alpha_{n-1} f_{n-1}(\alpha_n^{-1} \alpha_{n-1}^{-1} x)),$$

$$f_{n+1}(x) = \alpha_n \alpha_{n-1} f_{n-1}(\alpha_{n-1}^{-1} f_n(\alpha_n^{-1} x)).$$

Then, taking limits at $n \to \infty$ we have that the statements (1) and (2) imply that

(3) The universal function f_* is a solution of the functional equations

$$f_*(x) = \alpha_* f_*(\alpha_* f_*(\alpha_*^{-2} x)), \qquad f_*(x) = \alpha_*^2 f_*(\alpha_*^{-1} f_*(\alpha_*^{-2} x)).$$

Moreover, it turns out that f_* is an analytic function in x^{2k+1} (we refer for example to [40]).

Remark 5.3 For the cubic critical case, there are unpublished computer-assisted proofs (we refer to [34, 36]) that establish the existence of the universal function f_* .

Definition 5.4 Given a critical map f as in Definition 2.5, we introduce

$$\Lambda(x,n) = \sum_{j=1}^{n} (f^{n-j})' \circ f^{j}(x).$$

It is straightforward to check that

$$\Lambda(x, m+n) = (f^m)' \circ f^n(x)\Lambda(x, n) + \Lambda(f^n(x), m). \tag{27}$$

A renormalization scheme for Λ follows from introducing $\lambda_{(n)}(x) = \Lambda(x, F_n)$ and using (27), $F_n = F_{n-1} + F_{n-2}$ and $f_{(n)}(x) = f^{F_n}(x) - F_{n-1}$, thus obtaining

$$\lambda_{(n)}(x) = f'_{(n-1)} \circ f_{(n-2)}(x) \lambda_{(n-2)}(x) + \lambda_{(n-1)}(f_{(n-2)}(x)).$$

Then, after the scaling $\lambda_n(x) = \lambda_{(n)}(\alpha_{n-1}^{-1}x)$, we introduce the following operators (which are called *Lindeberg-Lyapunov operators*)

$$\begin{pmatrix} \lambda_n \\ \lambda_{n-1} \end{pmatrix} = \mathcal{K}_n \cdots \mathcal{K}_1 \begin{pmatrix} \lambda_2 \\ \lambda_1 \end{pmatrix}, \quad \mathcal{K}_n = \begin{pmatrix} \mathcal{L}_n & \mathcal{M}_n \\ \mathrm{id} & 0 \end{pmatrix}$$

given by

$$\mathcal{L}_n[\lambda](x) := f'_{n-1}(\alpha_{n-2}f_{n-2}(\alpha_{n-1}\alpha_{n-2}x))\lambda(\alpha_{n-1}^{-1}\alpha_{n-2}^{-1}x),$$

$$\mathcal{M}_n[\lambda](x) := \lambda(\alpha_{n-2}f_{n-2}(\alpha_{n-1}^{-1}\alpha_{n-2}^{-1}x)).$$

As it is discussed in [5, 6], an important consequence of the exponential convergence of f_n to f_* is that the Lindeberg-Lyapunov operators \mathcal{K}_n converge exponentially fast to an operator \mathcal{K}_* as $n \to \infty$. Moreover, the operators \mathcal{K}_n are compact in an appropriate space of analytic functions and they preserve the cone of pairs of complex functions, such that their components are strictly positive when restricted to the reals. Hence, we can apply Kreı̆n-Rutman theorem (see for example [45]) an obtain that

Theorem 5.5 Let us consider a critical circle map of order 2k + 1, having rotation number $\rho(f) = \theta = \frac{\sqrt{5}-1}{2}$, as described in Definition 2.5. Denote by $\mathcal{K}_{\infty} = \mathcal{K}_{*}$ and let ρ_{n} be the spectral radius of the operators \mathcal{K}_{n} for every $n \in \mathbb{N} \cup \{\infty\}$. Then,

- ρ_n is a positive eigenvalue of \mathcal{K}_n .
- The rest of spec(\mathcal{K}_n)\{0} consists of eigenvalues whose modulus is less than ρ_n .
- A pair of positive functions (ψ_n, ϕ_n) is an eigenvector of \mathcal{K}_n if and only if the corresponding eigenvalue is ρ_n .
- We have that $\rho_* > \alpha_*^{2k} > 1$ and that there is a constant c > 0 such that for all positive pairs of functions (λ_1, λ_2) we have

$$c^{-1}\rho_*^n \leq \lambda_n(x) \leq c\rho_*^n, \qquad {\lambda_n \choose \lambda_{n-1}} = \mathcal{K}_n \cdots \mathcal{K}_1 {\lambda_2 \choose \lambda_1}.$$

Proof This statements are justified in [5, 6] specifying also the corresponding domains of definition which are not discussed here.

Now, let us make use of Theorem 5.5 to characterize the growth of the derivatives of the rotation number at the tip of Arnold tongues. To this end, we consider the 2-parameter family of maps $(\omega, \varepsilon) \mapsto f_{\omega,\varepsilon}$ given by (5), and we observe that the derivatives with respect to ω and ε of the iterates of the map $f_{\omega,\varepsilon}$ are written as (in order to simplify the notation we omit the dependence on ω and ε in the map)

$$D_{\mu}[f^n](x) = \sum_{j=1}^n (f^{n-j})' \circ f^j(x) \xi_{\mu} \circ f^j(x), \quad \mu = \omega, \varepsilon$$



where (of course these computations are valid for any family of maps satisfying similar properties as (5))

$$\xi_{\omega}(x) = \partial_{\omega} f(x) = 1, \qquad \xi_{\varepsilon}(x) = \partial_{\varepsilon} f(x) = \frac{1}{2\pi} \sin(2\pi x).$$
 (28)

Let us observe that we have an analogous of (27), which is given by

$$D_{\mu}[f^{m+n}](x) = (f^m)' \circ f^n(x) D_{\mu}[f^n](x) + D_{\mu}[f^m] \circ f^n(x)$$
(29)

and also that there exist constants $c_1, c_2 > 0$ that allow us to control $D_{\mu}[f^n]$ as follows

$$c_1\Lambda(x,n) < |D_{\mu}[f^n](x)| < c_2\Lambda(x,n), \quad \mu = \omega, \varepsilon.$$

Therefore, using the properties of Theorem 5.5, we obtain (at $\varepsilon = 1$)

$$c_1c^{-1}\rho_*^n \le |D_\mu[f^{F_n}](x)| \le c_2c\rho_*^n, \quad \mu = \omega, \varepsilon,$$

thus concluding that (at $\varepsilon = 1$)

$$\left| \frac{D_{\varepsilon}[f^n](x)}{D_{\omega}[f^n](x)} \right| \le c_2 c_1^{-1}.$$

Remark 5.6 For the particular example of the Arnold family, we have that the expressions (28) allow us to write

$$D_{\omega}[f^n](x) = \Lambda(x, n), \qquad |D_{\varepsilon}[f^n](x)| \le \frac{1}{2\pi} \cdot \Lambda(x, n)$$

thus obtaining a theoretical bound $|\omega'(1)| \le 0.159155$. Indeed, the computations presented in Fig. 2 show that $|\omega'(1)| \simeq 0.01748...$

5.2 Geometric Interpretation and Bound of the Differentiability

To describe a global picture of the renormalization group we need to take into account the dependence on the rotation number. For the purposes of the present paper, it suffices to recall the construction in [40] based on commuting pairs. In the following, we will consider renormalization both in the space of analytic diffeomorphisms and in the space of analytic cubic critical maps.

The renormalization group transformation \mathcal{R}_m , applied to a particular circle homeomorphism f depends upon m, where m is such that $m \le 1/\rho(f) < m+1$ —in other words, m is the first term in the continued fraction of $\rho(f)$. This transformation is introduced as follows:

Definition 5.7 Consider the space φ_m of pairs (ξ, η) of analytic homeomorphisms of \mathbb{R} which satisfy the following conditions

- (1) $\xi(0) = \eta(0) + 1$.
- (2) $\eta(\xi(0)) = \xi(\eta(0)).$
- (3) $0 < \xi(0) < 1$.
- (4) $\xi^m(\eta(0)) > 0$.
- (5) $\xi^{m-1}(\eta(0)) < 0$.



- (6) If $\xi'(x) = 0$ or $\eta'(x) = 0$ for $x \in [\eta(0), \xi(0)]$, then x = 0 and $\eta'(0) = \xi'(0) = \eta''(0) = \xi'''(0) = 0$, but $\xi'''(0)$ and $\eta'''(0)$ are nonzero.
- (7) $(\xi \eta)'(0) = (\eta \xi)'(0)$, and if $\xi'(0) = 0$, then $(\xi \eta)'''(0) = (\eta \xi)'''(0)$.

Then, the renormalization map \mathcal{R}_m acting on φ_m is defined by

$$\mathcal{R}_m(\xi(x), \eta(x)) = (\alpha \xi^{m-1}(\eta(x/\alpha)), \alpha \xi^{m-1}(\eta(\xi(x/\alpha)))),$$

where $\alpha = 1/(\xi^{m-1}(\eta(0)) - \xi^m(\eta(0)))$.

This construction—using conditions (1), (2) and (3)—allows us to associate a homeomorphism $f = f_{\xi,\eta}$ on the unit circle to each pair $(\xi,\eta) \in \varphi_m$ by defining $f = \xi$ on $[\eta(0),0]$ and $f = \eta$ on $[0,\xi(0)]$ and identifying the end points of the interval $[\eta(0),\xi(0)]$. Conditions (4) and (5) guarantee that the rotation number of this circle map satisfies $m \le 1/\rho(f_{\xi,\eta}) < m+1$ and also that $\alpha < -1$. Furthermore, it is not difficult to see that conditions (1), (2), (3), (6) and (7) are preserved by \mathcal{R}_m .

Analytic diffeomorphisms $\operatorname{Diff}_+^{\omega}(\mathbb{T})$ and cubic critical maps \mathfrak{C}^3 are embedded in the space $\bigcup_{m\in\mathbb{N}}\varphi_m$ just by considering the map $f\mapsto (f,f-1)$. Notice also that, according with Definition 2.5, we can think of \mathfrak{C}^3 as a cell of lower dimension, invariant under the action of \mathcal{R}_m , attached to the boundary of the space of circle maps.

The behavior of the rotation number under the action of the renormalization transformation is characterized in the following Lemma (we refer to [40] for details)

Lemma 5.8 If
$$m \le \rho(f_{\xi,\eta}) < m+1$$
, then $\rho(f_{\mathcal{R}_m(\xi,\eta)}) = 1/\rho(f_{\xi,\eta}) - m$.

An immediate consequence of this result is the following: a map $f \in \text{Diff}_+^{\omega}(\mathbb{T})$ (respectively $f \in \mathfrak{C}^3$) has golden mean rotation number $\rho(f) = \theta = \frac{\sqrt{5}-1}{2}$ if and only if $\mathcal{R}_1(f)$ does. Consequently, the spaces

$$\{f\in \operatorname{Diff}^\omega_+(\mathbb{T}): \rho(f)=\theta\} \quad \text{and} \quad \{f\in \mathfrak{C}^3: \rho(f)=\theta\}$$

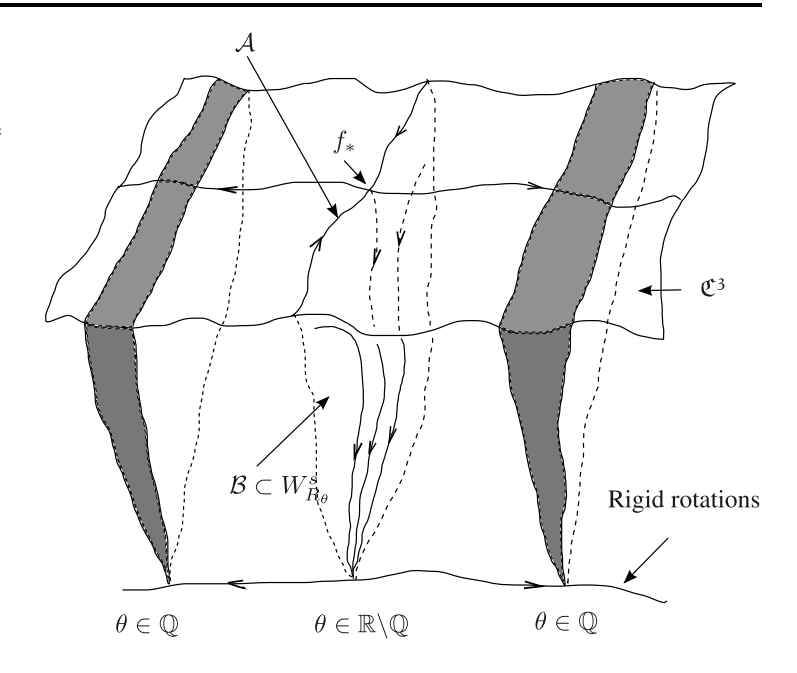
are invariant under \mathcal{R}_1 (actually, the restriction of the transformation \mathcal{R}_1 coincides with the local transformation \mathcal{R} , given by (25), described in the previous section). Notice that we are restricting the discussion for the golden mean but other rotation numbers can be considered. Indeed, Lemma 5.8 motivates that if the continued fraction of the studied rotation number is eventually periodic, then it makes sense to search for a fixed point in the renormalization group transformation.

Now, let us describe the geometric picture (see Fig. 5) corresponding to the action of the renormalization transformation \mathcal{R}_1 just introduced. Firstly, let us recall (see Remark 5.3) that in the space of cubic critical maps there is a fixed point f_* of the renormalization group (usually called the *non-trivial* of *strong-coupling* fixed point). Secondly, in the space of non-critical circle maps there is another fixed point (usually called *trivial* or *weak-coupling* fixed point), given by $R_{\theta}(x) = x + \theta$. Concretely:

- The non-trivial fixed point f_* is hyperbolic, having a two-dimensional unstable manifold which is a universal 2-parameter family of circle maps and contains the curve of rigid rotations in its closure. Moreover, the stable manifold of f_* has codimension two and consists of all elements of \mathfrak{C}^3 with rotation number θ .
- The trivial fixed point R_{θ} has a one-dimensional unstable manifold given by the curve of rigid rotations. Moreover, the stable manifold of R_{θ} has codimension one and consists of



Fig. 5 Picture of the renormalization group acting on the space of analytic circle maps with a critical boundary. \mathcal{A} is the stable manifold of the non-trivial fixed point f_* restricted to the critical space. \mathcal{B} is the slow unstable manifold of \mathcal{A}



all non-critical maps with rotation number θ . Let us observe that this stable manifold gets arbitrarily close to the non-trivial fixed point. Notice that, recalling Herman's Theorem, all the non-critical maps of rotation number θ must converge to the trivial fixed point under renormalization.

The spectrum of the linearized transformation at f_* restricted to the tangent space of \mathfrak{C}^3 consists of an eigenvalue δ , with $|\delta| > 1$ and a countable number of eigenvalues of modulus less than one. In addition, one can see that the eigenspace associated to δ is transverse to the subspace of maps of rotation number θ . The remaining unstable direction, which is transverse to \mathfrak{C}^3 , corresponds to an eigenvalue γ , with $|\delta| > |\gamma| > 1$.

Call $A = W_{f_*}^s \cap \mathfrak{C}^3$ the stable manifold of f_* in the critical space and call \mathcal{B} the slow unstable manifold of \mathcal{A} (associated to γ).

Remark 5.9 We recall that the slow unstable manifolds are manifolds associated to the eigenvector that increases the slowest decreasing eigenvalue. These manifolds have been considered in the mathematical literature. They have somewhat unexpected properties even in the finite dimensional case. A treatment that includes a discussion of the relations with β functions of renormalization is [11]. A treatment leading to a different manifold is [13]. More modern treatments appear in [3, 4].

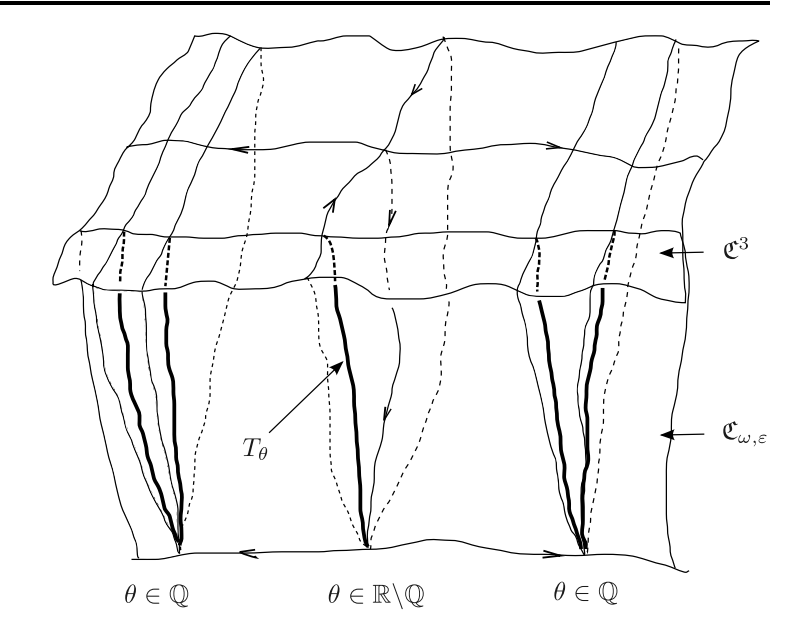
Notice that \mathcal{B} is invariant under renormalization and, since it is not contained in \mathfrak{C}^3 , it consists in maps having rotation number golden mean. Hence, $\mathcal{B} \subset W_{R_{\theta}}^s$, where $W_{R_{\theta}}^s$ in the stable manifold of R_{θ} under \mathcal{R}_1 (otherwise contradicting Herman's Theorem). Therefore, from Fenichel's theory of normally hyperbolic invariant manifolds under rate conditions (we refer to [20]) we conclude that the regularity of \mathcal{B} is C^r , with

$$r \ge \frac{\log \delta}{\log \gamma}, \qquad |\delta| > |\gamma| > 1.$$

Of course, this bound for the regularity of \mathcal{B} makes sense only at the boundary with the critical manifold, since $W_{R_0}^s$ is an analytic manifold.



Fig. 6 Arnold tongues of rotation number θ are obtained by intersecting the invariant manifold \mathcal{B} with a given two-parametric family $\mathfrak{C}_{\omega,\varepsilon}$ of circle maps



In general, r is only upper bound for the regularity but in many cases it is sharp. Notice also that this is a universal number since it depends only on the spectrum of the renormalization operator.

Finally, we observe that Arnold tongues, curves of constant rotation number, are obtained by intersecting the manifold \mathcal{B} with a given two-parametric family $\mathfrak{C}_{\omega,\varepsilon}$ of circle maps (see Fig. 6), chosen in such a way that $\mathfrak{C}_{\omega,0} = \{R_{\omega}, \ \omega \in [0,1)\}$ and $\mathfrak{C}_{\omega,1} \subset \mathfrak{C}^3$. Then, we identify the Arnold tongue T_{θ} with $\{f \in \mathfrak{C}_{\omega,\varepsilon} \cap \mathcal{B} : \rho(f) = \theta\}$.

Remark 5.10 For the case of $\theta = \frac{\sqrt{5}-1}{2}$, we have that $\delta \simeq 2.83362...$ and $\gamma = \alpha^2 \simeq 1.6604242...$. This values predict that the Arnold tongue is $\mathcal{C}^{2+0.05...}$.

Remark 5.11 Of course, the properties discussed in this section are generic. For particular families of circle maps we can observe higher regularity depending for example if we fall in a submanifold of \mathcal{A} with stronger stable eigenvalues.

6 Further Numerical Investigations

To enhance the universality of the results observed in Sect. 4 and the explanations reported in Sect. 5, we present additional computations related to Arnold tongues performed by means of Algorithms 3.2 and 3.5. We think that the large amount of computations shown in this section illustrates that both numerical methods are very efficient, fast and robust.

Along this section we consider families $(\omega, \varepsilon) \mapsto f_{\omega,\varepsilon}$ given by (5), (6), (7) and (8) for several values of the parameter κ . We recall that $f_{\omega,\varepsilon} \in \operatorname{Diff}_+^{\omega}(\mathbb{T})$ if $\varepsilon < 1$ and, depending of the parameter κ , we have that $f_{\omega,1} \in \mathfrak{C}^3$, \mathfrak{C}^5 or \mathfrak{C}^7 . For fixed rotation numbers that define Arnold tongues, we have selected quadratic irrationals of the form $\theta_{a,b} = (\sqrt{b^2 + 4b/a} - b)/2$, for $1 \le a \le b \le 5$, that have periodic continued fraction given by $\theta_{a,b} = [0; a,b,a,b,\ldots]$. It is clear that $\theta_{a,b} \in \mathcal{D}(C,2)$ for every a,b, but with a smaller constant C when a and b increase.



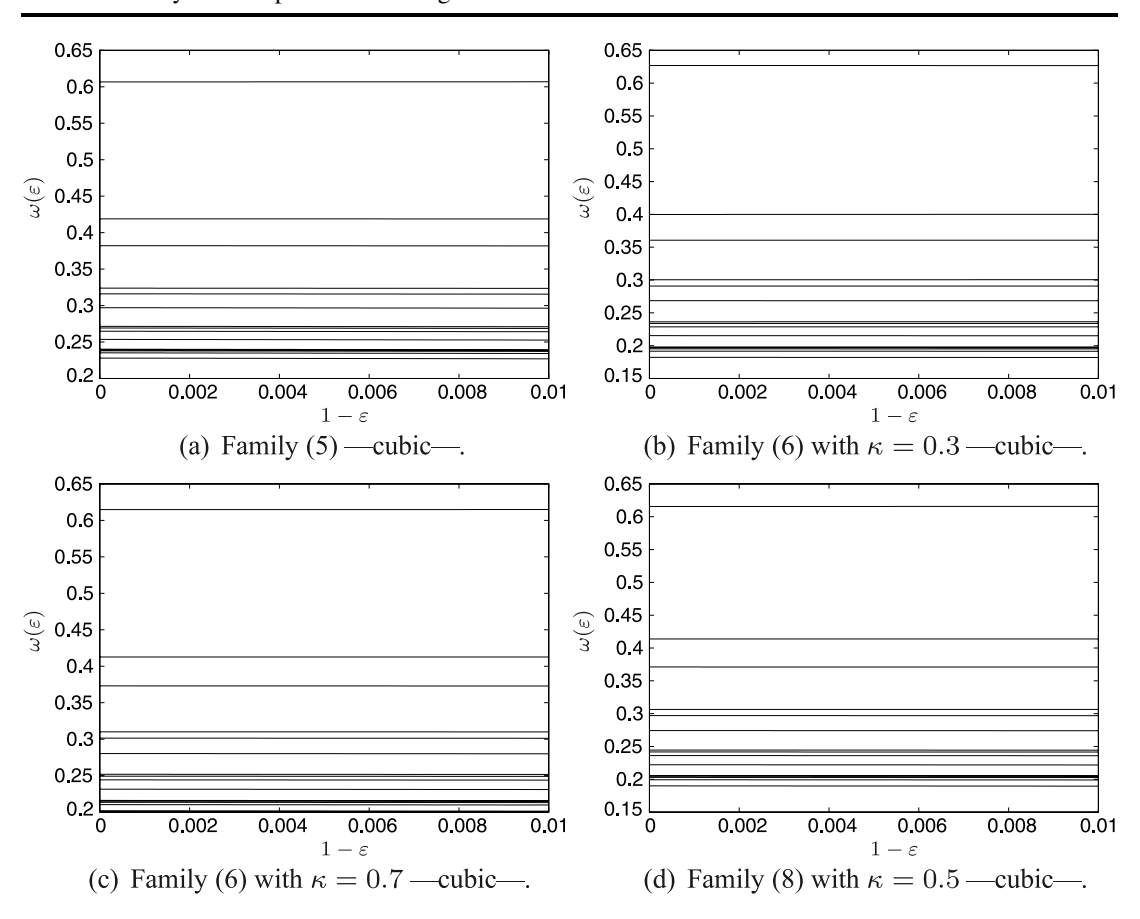


Fig. 7 Graph of $(1 - \varepsilon) \mapsto \omega(\varepsilon)$, close to the critical point for several families. Tongues in the plots correspond to $\theta_{a,b}$ for $1 \le a \le b \le 5$

6.1 Additional Computations of Arnold Tongues

As implementation parameters for Algorithm 3.2 we take an averaging order p=7 and $N=2^q$ iterates of the map, with $q \le 22$, asking for tolerances of 10^{-23} in the computation of the rotation number and 10^{-26} in the convergence of the secant method. Computations have been performed using 32-digit arithmetics (provided by the double-double data type from [26]). The continuation points are taken as $\varepsilon = 1 - 0.933254^n$, for $n = 0, 1, \ldots, 100$. As in Sect. 4, these selected points approach exponentially fast to the critical point, in order to obtain equispaced points in logarithmic scale.

In Figs. 7 and 8 we show the computed Arnold tongues $\varepsilon \mapsto \omega(\varepsilon)$ close to the critical points. The plots in Fig. 7 correspond to cubic families while those in Fig. 8 correspond to quintic and septic families. We observe that all these curves are clearly differentiable. Indeed, in Figs. 9 and 10 we plot the corresponding derivatives $\varepsilon \mapsto \omega'(\varepsilon)$.

The computed values $\omega(1)$ and $\omega'(1)$ of these Arnold tongues are given in Tables 1 and 2. We point out that some of the values $\omega(1)$ were also provided in [16] for the golden mean $\theta = (\sqrt{5} - 1)/2$, using the method in [47]. Of course we obtain the same results, even though it is worth mentioning that the method in [46] is much faster, since evaluating the interval phase locking for the continued fraction of the rotation number is not required. Precisely, this is the reason why we can systematically carry this study for different rotation numbers in a straightforward way.

Then, as we advanced in Remark 4.2, all the Arnold tongues corresponding to these numbers are smoother than C^1 at the critical point. If we evaluate the expression (23) for



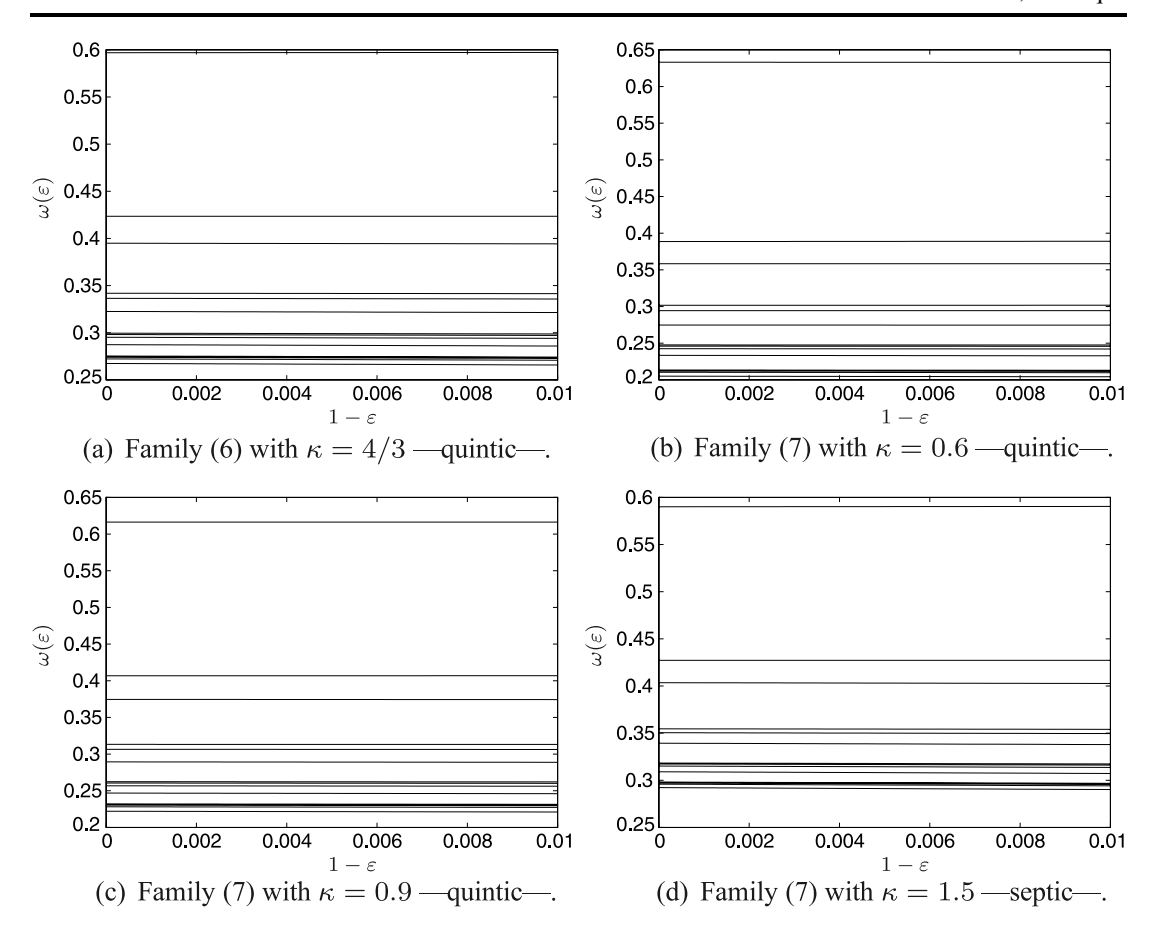


Fig. 8 Graph of $(1 - \varepsilon) \mapsto \omega(\varepsilon)$, close to the critical point for several families. Tongues in the plots correspond to $\theta_{a,b}$ for $1 \le a \le b \le 5$

these tongues, as it was done in Sect. 4, we observe that all of them either blow up or oscillate wildly. It is not surprising that the curve corresponding to the golden mean is the only one (among the computed rotation numbers) that is smoother than C^2 .

Let us recall that derivatives of the rotation number with respect to parameters blowup when we approach the critical point. Actually, renormalization group theory predicts an asymptotic expression of the form (here we use a generic parameter $\mu = \varepsilon, \omega$)

$$D_{\mu}\rho(\omega(\varepsilon),\varepsilon) \simeq \frac{\alpha_{\mu}}{(1-\varepsilon)^{\beta_{*}}} \left(1 + P_{\mu}(1-\varepsilon)\right) + \mathcal{O}\left(\frac{1}{(1-\varepsilon)^{\tilde{\beta}_{*}}}\right)$$
(30)

for certain constants α_{μ} , β_{*} , $\tilde{\beta}_{*}$ where the exponents $\beta_{*} > \tilde{\beta}_{*}$ depend only on the order of criticality and the rotation number. The function P_{μ} satisfies that $P_{\mu}(\delta(1-\varepsilon)) = P_{\mu}(1-\varepsilon)$, so it is periodic in logarithmic scale. Exponents β_{*} for the blow-up of the derivatives $D_{\omega}\rho$ and $D_{\varepsilon}\rho$ in the studied families are given in Tables 3 and 4, respectively.

In order to approximate this exponents we simply perform a linear fit at the derivatives in log-log scale, avoiding the oscillatory corrections mentioned before. Nevertheless, we observe a good agreement between exponents computed for the same rotation number and order of criticality. Notice also that we have consistent results corresponding to the exponents computed independently for $D_{\omega}\rho$ and $D_{\varepsilon}\rho$. We remark that the oscillatory terms increase with the order of criticality, making the fit of the results more complicated.

We want to stress again that both Algorithms 3.2 and 3.5 do not depend on the particular rotation number that we pretend to study. To illustrate this fact we consider the Arnold



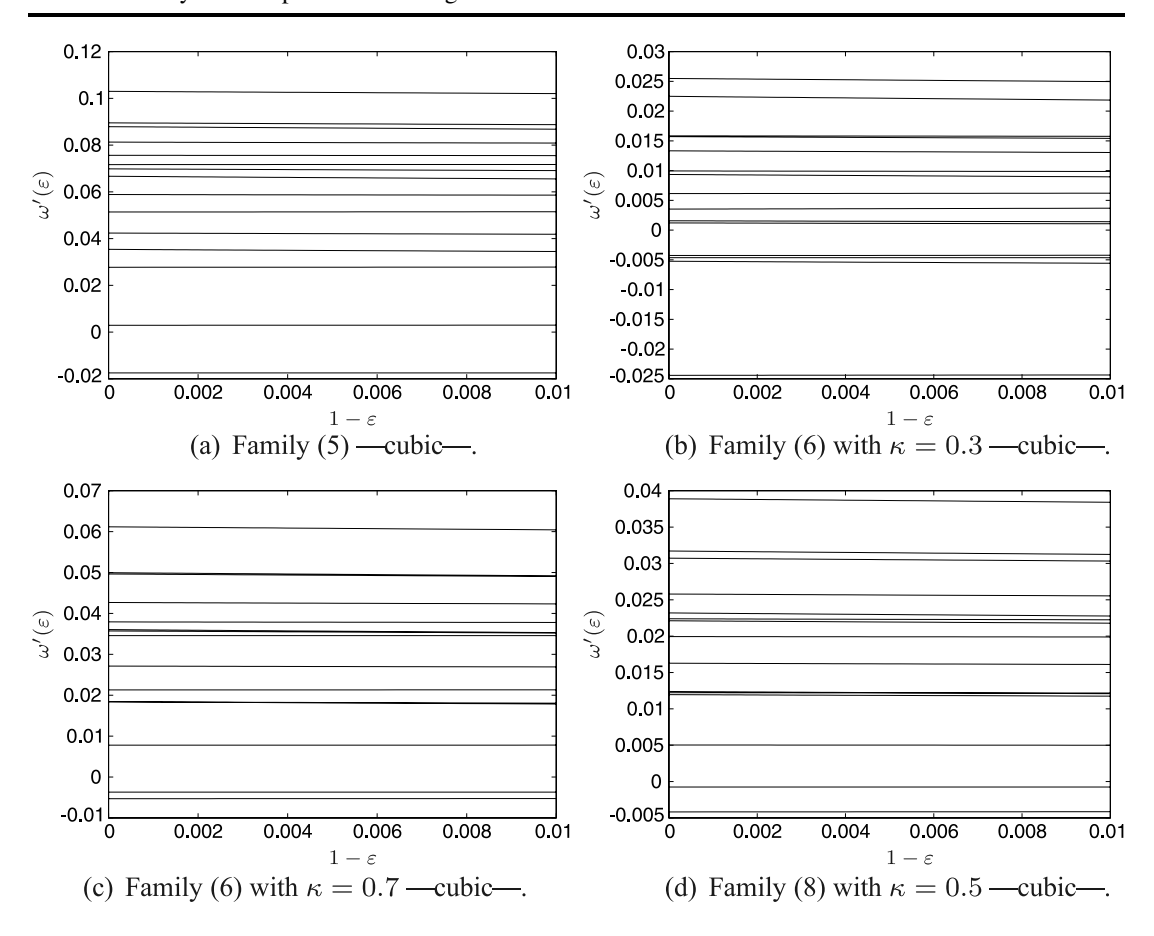


Fig. 9 Graph of the derivative $(1 - \varepsilon) \mapsto \omega'(\varepsilon)$, close to the critical point for several families. Tongues in the plots correspond to $\theta_{a,b}$ for $1 \le a \le b \le 5$

family (5) and we select different rotation numbers θ_n by taking 350 equispaced points in the interval $x_n \in [0, \pi/6]$ and $\theta_n = \sin(x_n) \in [0, 0.5]$. Since Diophantine numbers have large Lebesgue measure, we expect that the selected points have good arithmetic properties. However, we check this fact by computing the corresponding Brjuno function—given by (34)—and we accept the rotation number if $\mathcal{B}(\theta_n) \leq 4$.

Computations are performed using both Algorithms 3.2 and 3.5 obtaining the same results. The only difference is that the first one converges for $\varepsilon = 1$ and the second one does not, even though in the second case we can extrapolate very well the value $\omega(1)$ from the computed non-critical ones (recall that the curve is $\mathcal{C}^{1+\alpha}$).

The computed Arnold Tongues are shown in Fig. 11. Since the tongues approach each other when the parameter ε increases, we have different tones in the plot. The white zone corresponds to resonant Arnold tongues or phase-locking regions. Actually in [51] it was proved that the set of parameter values corresponding to irrational rotation numbers has zero Lebesgue measure and in [23] that it has Hausdorff dimension strictly smaller that one and greater or equal to 1/3. This is observed in Fig. 12 by plotting the singular density distribution of the Arnold tongues at the critical point, which is obtained using the program R for Statistical Computing [25]. The density of these tongues becomes singular at the critical point because the set of irrational Arnold tongues is a foliation which sends a set of positive measure into a set of zero measure.



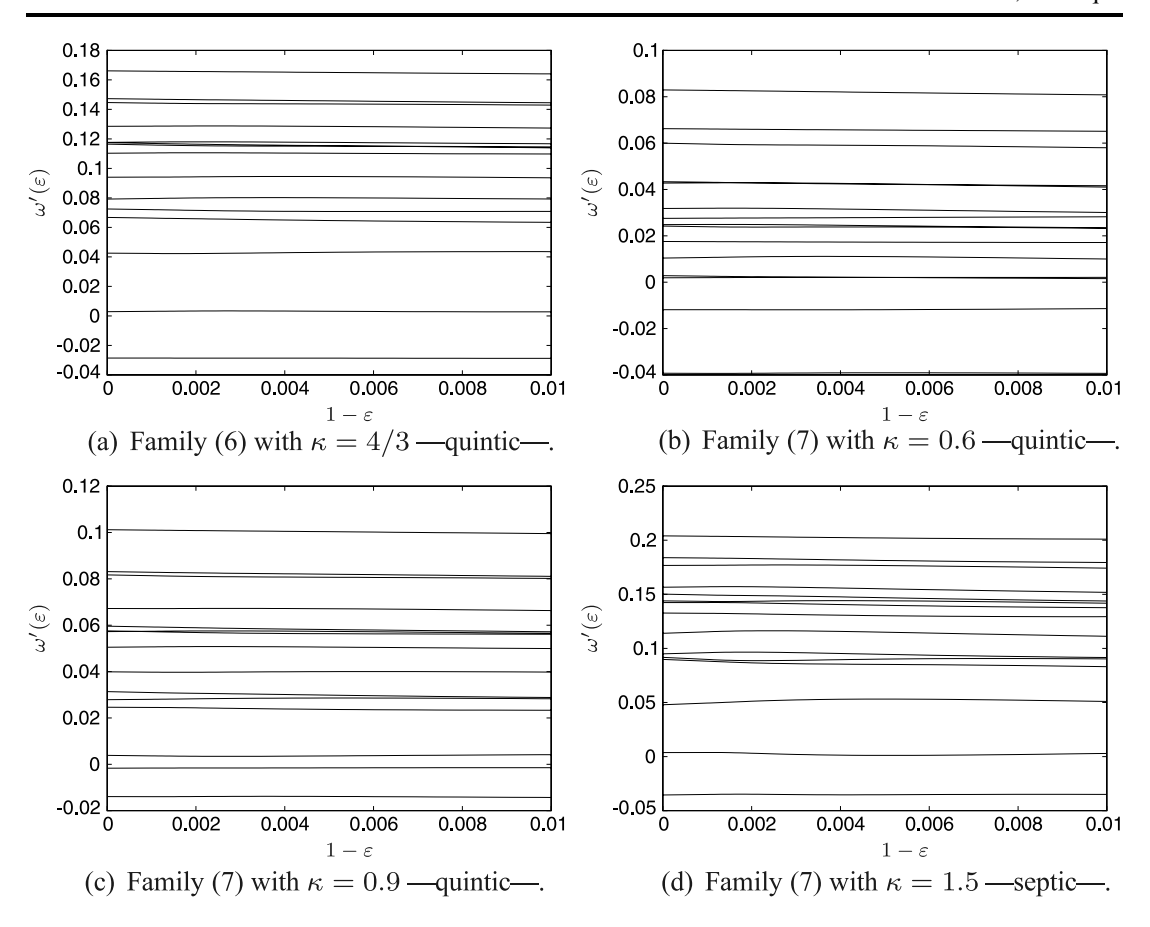


Fig. 10 Graph of the derivative $(1 - \varepsilon) \mapsto \omega'(\varepsilon)$, close to the critical point for several families. Tongues in the plots correspond to $\theta_{a,b}$ for $1 \le a \le b \le 5$

6.2 On the Breakdown of Sobolev Regularity

Now we present some computations using Algorithm 3.5 to illustrate the blow-up of Sobolev norms of conjugacies when approaching the critical point. Again, we consider the families $(\omega, \varepsilon) \mapsto f_{\omega,\varepsilon}$ given by (5), (6), (7) and (8) for several values of the parameter κ , and we fix rotations numbers of the form $\theta_{a,b} = (\sqrt{b^2 + 4b/a} - b)/2$, for $1 \le a \le b \le 5$.

The idea is to continue numerically these Arnold tongues monitoring the evolution of r-Sobolev norms of the conjugacy—see (20). Concretely, if $h_{\varepsilon}(x) = x + \xi_{\varepsilon}(x)$ is the conjugacy to a rigid rotation of the circle map $f_{\omega(\varepsilon),\varepsilon}$ satisfying $f_{\omega(\varepsilon),\varepsilon} \circ h_{\varepsilon} = h_{\varepsilon} \circ R_{\theta}$, then we compute the values $\|\xi_{\varepsilon}\|_r$ for 100 points $r \in [0, 2]$.

In Fig. 13 we plot some of the computed norms in order to illustrate their blow up. Then, in a similar way as discussed in relation with expressions (30), we fit the first order term of the following law

$$\|\xi_{\varepsilon}\|_{r} \simeq \frac{A_{*}(r)}{(1-\varepsilon)^{B_{*}(r)}} \left(1 + P_{*}(1-\varepsilon)\right) + \mathcal{O}\left(\frac{1}{(1-\varepsilon)^{\tilde{B}_{*}(r)}}\right),\tag{31}$$

for some constants $A_*(r)$, $B_*(r)$, where $B_*(r)$ is a universal number in the sense that depends only on the rotation number and the order of criticality. Some computations are given in Table 5.

We want to point out that (31) can be related to the renormalization group, thus obtaining a heuristic formula for the prediction for the exponents $B_*(r)$ in terms of the scaling proper-



Table 1 Critical values $\omega(1)$ for several rotation numbers and families

θ	Family (5)	Family (6), $\kappa = 0.3$	Family (6), $\kappa = 0.7$	Family (6), $\kappa = 4/3$
[0; 1, 1, 1, 1,]	0.60666106347011	0.62687105954673	0.61481318525291	0.59694625982733
$[0; 2, 1, 2, 1, \ldots]$	0.38212565637946	0.36062325061216	0.37308969032734	0.39491140275142
$[0; 2, 2, 2, 2, \ldots]$	0.41886498641897	0.39990316709114	0.41264132947169	0.42351776623671
$[0; 3, 1, 3, 1, \ldots]$	0.29707881009281	0.26853619235278	0.28029724322956	0.32257130250643
$[0; 3, 2, 3, 2, \ldots]$	0.31609640893852	0.29086464077852	0.30142766673575	0.33649021671957
$[0; 3, 3, 3, 3, \ldots]$	0.32387366602535	0.30045276849149	0.31006848017653	0.34187333729677
$[0; 4, 1, 4, 1, \ldots]$	0.25358922337337	0.21528631778779	0.23144008299429	0.28735985806134
$[0; 4, 2, 4, 2, \ldots]$	0.26481615381242	0.22870487487661	0.24423747695879	0.29518260647474
$[0; 4, 3, 4, 3, \ldots]$	0.26924114574461	0.23383349744976	0.24927706959563	0.29809076070052
$[0; 4, 4, 4, 4, \ldots]$	0.27150235886599	0.23639389072267	0.25185893948316	0.29950445821370
$[0; 5, 1, 5, 1, \ldots]$	0.22798444384638	0.18222910335518	0.20189602203919	0.26743847255173
$[0; 5, 2, 5, 2, \ldots]$	0.23517195185003	0.19163068831675	0.21026572304927	0.27225731561090
$[0; 5, 3, 5, 3, \ldots]$	0.23793193615175	0.19519345236594	0.21347535861221	0.27399967886214
$[0; 5, 4, 5, 4, \ldots]$	0.23932398378781	0.19699876644569	0.21509641059390	0.27483473261402
$[0; 5, 5, 5, 5, \ldots]$	0.24012917730632	0.19805419119542	0.21603622555704	0.27529864834701
θ	Family (8), $\kappa = 0.5$	Family (7), $\kappa = 0.6$	Family (7), $\kappa = 0.9$	Family (7), $\kappa = 1.5$
$\frac{\theta}{[0;1,1,1,1,\ldots]}$	Family (8), $\kappa = 0.5$ 0.61567565128166	Family (7), $\kappa = 0.6$ 0.63313304089504	Family (7), $\kappa = 0.9$ 0.61633050179571	Family (7), $\kappa = 1.5$ 0.59005254922276
	•	• • •	•	
[0; 1, 1, 1, 1,]	0.61567565128166	0.63313304089504	0.61633050179571	0.59005254922276
[0; 1, 1, 1, 1,] [0; 2, 1, 2, 1,]	0.61567565128166 0.37113750513616	0.63313304089504 0.35835245630167	0.61633050179571 0.37459080295573	0.59005254922276 0.40351729363417
$[0; 1, 1, 1, 1, \dots]$ $[0; 2, 1, 2, 1, \dots]$ $[0; 2, 2, 2, 2, \dots]$	0.61567565128166 0.37113750513616 0.41381227245236	0.63313304089504 0.35835245630167 0.38862276635541	0.61633050179571 0.37459080295573 0.40674475830016	0.59005254922276 0.40351729363417 0.42724158766426
[0; 1, 1, 1, 1,] [0; 2, 1, 2, 1,] [0; 2, 2, 2, 2,] [0; 3, 1, 3, 1,]	0.61567565128166 0.37113750513616 0.41381227245236 0.27421337809363	0.63313304089504 0.35835245630167 0.38862276635541 0.27479777089192	0.61633050179571 0.37459080295573 0.40674475830016 0.28941098812035	0.59005254922276 0.40351729363417 0.42724158766426 0.33935075990077
[0; 1, 1, 1, 1,] [0; 2, 1, 2, 1,] [0; 2, 2, 2, 2,] [0; 3, 1, 3, 1,] [0; 3, 2, 3, 2,]	0.61567565128166 0.37113750513616 0.41381227245236 0.27421337809363 0.29703674674343	0.63313304089504 0.35835245630167 0.38862276635541 0.27479777089192 0.29439459617477	0.61633050179571 0.37459080295573 0.40674475830016 0.28941098812035 0.30653889725553	0.59005254922276 0.40351729363417 0.42724158766426 0.33935075990077 0.35045111426901
[0; 1, 1, 1, 1,] [0; 2, 1, 2, 1,] [0; 2, 2, 2, 2,] [0; 3, 1, 3, 1,] [0; 3, 2, 3, 2,] [0; 3, 3, 3, 3,]	0.61567565128166 0.37113750513616 0.41381227245236 0.27421337809363 0.29703674674343 0.30642250791340	0.63313304089504 0.35835245630167 0.38862276635541 0.27479777089192 0.29439459617477 0.30167316749381	0.61633050179571 0.37459080295573 0.40674475830016 0.28941098812035 0.30653889725553 0.31326694792198	0.59005254922276 0.40351729363417 0.42724158766426 0.33935075990077 0.35045111426901 0.35457863104247
[0; 1, 1, 1, 1,] [0; 2, 1, 2, 1,] [0; 2, 2, 2, 2,] [0; 3, 1, 3, 1,] [0; 3, 2, 3, 2,] [0; 3, 3, 3, 3, 3,]	0.61567565128166 0.37113750513616 0.41381227245236 0.27421337809363 0.29703674674343 0.30642250791340 0.22212813733449	0.63313304089504 0.35835245630167 0.38862276635541 0.27479777089192 0.29439459617477 0.30167316749381 0.23346214811924	0.61633050179571 0.37459080295573 0.40674475830016 0.28941098812035 0.30653889725553 0.31326694792198 0.24684360339516	0.59005254922276 0.40351729363417 0.42724158766426 0.33935075990077 0.35045111426901 0.35457863104247 0.30902598272223
[0; 1, 1, 1, 1,] [0; 2, 1, 2, 1,] [0; 2, 2, 2, 2,] [0; 3, 1, 3, 1,] [0; 3, 2, 3, 2,] [0; 3, 3, 3, 3, 3,] [0; 4, 1, 4, 1,] [0; 4, 2, 4, 2,]	0.61567565128166 0.37113750513616 0.41381227245236 0.27421337809363 0.29703674674343 0.30642250791340 0.22212813733449 0.23613533662923	0.63313304089504 0.35835245630167 0.38862276635541 0.27479777089192 0.29439459617477 0.30167316749381 0.23346214811924 0.24254965099543	0.61633050179571 0.37459080295573 0.40674475830016 0.28941098812035 0.30653889725553 0.31326694792198 0.24684360339516 0.25677909160315	0.59005254922276 0.40351729363417 0.42724158766426 0.33935075990077 0.35045111426901 0.35457863104247 0.30902598272223 0.31510031370341
[0; 1, 1, 1, 1,] [0; 2, 1, 2, 1,] [0; 2, 2, 2, 2,] [0; 3, 1, 3, 1,] [0; 3, 2, 3, 2,] [0; 4, 1, 4, 1,] [0; 4, 2, 4, 2,] [0; 4, 3, 4, 3,]	0.61567565128166 0.37113750513616 0.41381227245236 0.27421337809363 0.29703674674343 0.30642250791340 0.22212813733449 0.23613533662923 0.24165845987386	0.63313304089504 0.35835245630167 0.38862276635541 0.27479777089192 0.29439459617477 0.30167316749381 0.23346214811924 0.24254965099543 0.24599201459714	0.61633050179571 0.37459080295573 0.40674475830016 0.28941098812035 0.30653889725553 0.31326694792198 0.24684360339516 0.25677909160315 0.26053229443740	0.59005254922276 0.40351729363417 0.42724158766426 0.33935075990077 0.35045111426901 0.35457863104247 0.30902598272223 0.31510031370341 0.31726556639141
[0; 1, 1, 1, 1,] [0; 2, 1, 2, 1,] [0; 2, 2, 2, 2,] [0; 3, 1, 3, 1,] [0; 3, 2, 3, 2,] [0; 4, 1, 4, 1,] [0; 4, 2, 4, 2,] [0; 4, 3, 4, 3,] [0; 4, 4, 4, 4, 4,]	0.61567565128166 0.37113750513616 0.41381227245236 0.27421337809363 0.29703674674343 0.30642250791340 0.22212813733449 0.23613533662923 0.24165845987386 0.24450197931748	0.63313304089504 0.35835245630167 0.38862276635541 0.27479777089192 0.29439459617477 0.30167316749381 0.23346214811924 0.24254965099543 0.24599201459714 0.24766934120454	0.61633050179571 0.37459080295573 0.40674475830016 0.28941098812035 0.30653889725553 0.31326694792198 0.24684360339516 0.25677909160315 0.26053229443740 0.26238374706392	0.59005254922276 0.40351729363417 0.42724158766426 0.33935075990077 0.35045111426901 0.35457863104247 0.30902598272223 0.31510031370341 0.31726556639141 0.31828876978394
[0; 1, 1, 1, 1,] [0; 2, 1, 2, 1,] [0; 2, 2, 2, 2,] [0; 3, 1, 3, 1,] [0; 3, 2, 3, 2,] [0; 4, 1, 4, 1,] [0; 4, 2, 4, 2,] [0; 4, 3, 4, 3,] [0; 4, 4, 4, 4, 4,] [0; 5, 1, 5, 1,]	0.61567565128166 0.37113750513616 0.41381227245236 0.27421337809363 0.29703674674343 0.30642250791340 0.22212813733449 0.23613533662923 0.24165845987386 0.24450197931748 0.18996231415208	0.63313304089504 0.35835245630167 0.38862276635541 0.27479777089192 0.29439459617477 0.30167316749381 0.23346214811924 0.24254965099543 0.24599201459714 0.24766934120454 0.20506531290792	0.61633050179571 0.37459080295573 0.40674475830016 0.28941098812035 0.30653889725553 0.31326694792198 0.24684360339516 0.25677909160315 0.26053229443740 0.26238374706392 0.22204716742246	0.59005254922276 0.40351729363417 0.42724158766426 0.33935075990077 0.35045111426901 0.35457863104247 0.30902598272223 0.31510031370341 0.31726556639141 0.31828876978394 0.29222344245490
[0; 1, 1, 1, 1,] [0; 2, 1, 2, 1,] [0; 2, 2, 2, 2,] [0; 3, 1, 3, 1,] [0; 3, 2, 3, 2,] [0; 4, 1, 4, 1,] [0; 4, 2, 4, 2,] [0; 4, 3, 4, 3,] [0; 4, 4, 4, 4, 4,] [0; 5, 1, 5, 1,] [0; 5, 2, 5, 2,]	0.61567565128166 0.37113750513616 0.41381227245236 0.27421337809363 0.29703674674343 0.30642250791340 0.22212813733449 0.23613533662923 0.24165845987386 0.24450197931748 0.18996231415208 0.19928758150802	0.63313304089504 0.35835245630167 0.38862276635541 0.27479777089192 0.29439459617477 0.30167316749381 0.23346214811924 0.24254965099543 0.24599201459714 0.24766934120454 0.20506531290792 0.21038885255896	0.61633050179571 0.37459080295573 0.40674475830016 0.28941098812035 0.30653889725553 0.31326694792198 0.24684360339516 0.25677909160315 0.26053229443740 0.26238374706392 0.22204716742246 0.22814569979955	0.59005254922276 0.40351729363417 0.42724158766426 0.33935075990077 0.35045111426901 0.35457863104247 0.30902598272223 0.31510031370341 0.31726556639141 0.31828876978394 0.29222344245490 0.295895555394143

ties and the rotation number (we follow the arguments in [2]). To this end, we set $\lambda=1-\varepsilon$ and we consider the family of circle maps—for convenience, we omit the dependence on the parameter ω in the family—

$$f_{\lambda}(x) = x + \omega - \frac{1 - \lambda}{2\pi} g(2\pi x),$$

where g is a 1-periodic function, satisfying $g'(0) = 2\pi$, as in the examples given by (5), (6), (7) and (8). Notice that the critical point corresponds to $\lambda = 0$. The key observation is that



Table 2 Derivative $\omega'(1)$ for several rotation numbers and families

θ	Family (5)	Family (6), $\kappa = 0.3$	Family (6), $\kappa = 0.7$	Family (6), $\kappa = 4/3$
$[0; 1, 1, 1, 1, \dots]$	-0.017480008706	0.015844188888	-0.005297174685	-0.028545926033
$[0; 2, 1, 2, 1, \ldots]$	0.035398636056	-0.005231158488	0.018425583068	0.066785487700
$[0; 2, 2, 2, 2, \ldots]$	0.002917141025	-0.024409767066	-0.003682733151	0.002888830832
$[0; 3, 1, 3, 1, \ldots]$	0.066670897459	0.013323865197	0.036049987734	0.117467946576
$[0; 3, 2, 3, 2, \ldots]$	0.042388154205	0.001567670798	0.018392446240	0.072501615773
$[0; 3, 3, 3, 3, \ldots]$	0.027734098090	-0.004640726796	0.007791789630	0.042559444114
$[0;4,1,4,1,\ldots]$	0.087891436301	0.022485184504	0.049963021585	0.147292465097
$[0; 4, 2, 4, 2, \ldots]$	0.069844498563	0.009352515130	0.035722919701	0.116421906852
$[0;4,3,4,3,\ldots]$	0.058858174400	0.001208860914	0.027133714502	0.094025465075
$[0; 4, 4, 4, 4, \ldots]$	0.051387391565	-0.004267696674	0.021301234528	0.079185096802
$[0; 5, 1, 5, 1, \ldots]$	0.102996438306	0.025491194823	0.061178543520	0.166115191409
$[0; 5, 2, 5, 2, \ldots]$	0.089527362287	0.015715539045	0.049640825551	0.144658034280
$[0; 5, 3, 5, 3, \ldots]$	0.081292422821	0.009941703525	0.042680129321	0.128534409348
$[0; 5, 4, 5, 4, \ldots]$	0.075645185852	0.006143284836	0.037929898442	0.117664005496
$[0; 5, 5, 5, 5, \ldots]$	0.071653884023	0.003531956411	0.034574498276	0.110282140800
$\overline{\theta}$	Family (8), $\kappa = 1/2$	Family (7), $\kappa = 0.6$	Family (7), $\kappa = 0.9$	Family (7), $\kappa = 1.5$
$[0; 1, 1, 1, 1, \ldots]$	-0.004171196679	0.027537364113	-0.001674483085	-0.035470663937
$[0; 2, 1, 2, 1, \ldots]$	0.012391201596	0.002825329200	0.031358660599	0.089826694502
$[0; 2, 2, 2, 2, \ldots]$	-0.000748943517	-0.039280048359	-0.013909345625	0.003674506323
$[0; 3, 1, 3, 1, \ldots]$	0.023194322552	0.017569479600	0.059575574792	0.150212001091
$[0; 3, 2, 3, 2, \ldots]$	0.011959968014	0.001897136580	0.024632033662	0.091716021501
$[0; 3, 3, 3, 3, \ldots]$	0.005029281641	-0.011861643071	0.003861749221	0.047934287671
$[0; 4, 1, 4, 1, \ldots]$	0.031707953463	0.066236772883	0.083123456845	0.183890189357
$[0; 4, 2, 4, 2, \ldots]$	0.022116085364	0.043358356155	0.057560268438	0.143930363856
$[0;4,3,4,3,\ldots]$	0.016276476088	0.024207462318	0.039912128324	0.113977120621
$[0; 4, 4, 4, 4, \ldots]$	0.012222150602	0.010405137696	0.027873412931	0.095003522888
$[0; 5, 1, 5, 1, \ldots]$	0.038896089329	0.082957511062	0.101218153327	0.203990264191
$[0; 5, 2, 5, 2, \ldots]$	0.030722981151	0.059962122538	0.081693151984	0.176700904422
$[0; 5, 3, 5, 3, \ldots]$	0.025793951377	0.042755733323	0.067215229427	0.156571561027
$[0; 5, 4, 5, 4, \ldots]$	0.022388211725	0.031797997816	0.057242185950	0.142412448314
$[0; 5, 5, 5, 5, \ldots]$	0.019944270297	0.024829041191	0.050500445834	0.132656171032

renormalization sends

$$h_{\gamma\lambda}(x) \simeq \alpha_* h_{\lambda}(\sigma x),$$
 (32)

where α_* is the universal constant given in (26), γ is the eigenvalue of the non-trivial fixed point transversal to the critical space and σ is the exponent of convergence of the continued fraction of the fixed rotation number θ .

For example, we justify (32) for the case of the golden mean $\theta = (\sqrt{5} - 1)/2$ (in this case σ is known to be also the golden mean). To renormalize the map f_{λ} , for $\lambda \simeq 0$, we compute

$$f_{\lambda}^{F_n}(h_{\lambda}(x)) - F_{n-1} = h_{\lambda}(x + F_n\theta - F_{n-1}) \simeq h_{\lambda}(x + \theta^n)$$



Table 3 Exponent β_* in the blow-up of derivatives of the rotation number with respect to ω , for several rotation numbers and families

θ	Family (5)	Family (6	5)		Family (8)	Family (7)			
		$\kappa = 0.3$	$\kappa = 0.7$	$\kappa = 4/3$	$\kappa = 1/2$	$\kappa = 0.6$	$\kappa = 0.9$	$\kappa = 1.5$	
$[0; 1, 1, 1, 1, \dots]$	0.1552	0.1556	0.1550	0.2124	0.1557	0.2112	0.2114	0.2446	
$[0; 2, 1, 2, 1, \ldots]$	0.1749	0.1747	0.1748	0.2330	0.1739	0.2395	0.2323	0.2687	
$[0; 2, 2, 2, 2, \ldots]$	0.1660	0.1645	0.1659	0.2257	0.1665	0.2260	0.2283	0.2560	
$[0; 3, 1, 3, 1, \ldots]$	0.2060	0.2038	0.2057	0.2683	0.2048	0.2642	0.2670	0.2958	
$[0; 3, 2, 3, 2, \ldots]$	0.1811	0.1788	0.1806	0.2411	0.1795	0.2406	0.2430	0.2602	
$[0; 3, 3, 3, 3, \ldots]$	0.1871	0.1849	0.1865	0.2491	0.1858	0.2482	0.2476	0.2874	
$[0; 4, 1, 4, 1, \ldots]$	0.2382	0.2412	0.2385	0.2982	0.2386	0.2814	0.2985	0.3705	
$[0; 4, 2, 4, 2, \ldots]$	0.2021	0.2061	0.2019	0.2506	0.2015	0.2490	0.2561	0.2829	
$[0; 4, 3, 4, 3, \ldots]$	0.2035	0.2072	0.2031	0.2596	0.2021	0.2208	0.2485	0.3167	
$[0; 4, 4, 4, 4, \ldots]$	0.2151	0.2182	0.2142	0.2831	0.2136	0.2542	0.2761	0.3132	
$[0; 5, 1, 5, 1, \ldots]$	0.2702	0.2694	0.2700	0.3256	0.2708	0.3371	0.3293	0.3753	
$[0; 5, 2, 5, 2, \ldots]$	0.2259	0.2250	0.2255	0.2773	0.2248	0.2851	0.2794	0.3178	
$[0; 5, 3, 5, 3, \ldots]$	0.2226	0.2244	0.2237	0.2844	0.2241	0.2828	0.2741	0.3293	
$[0; 5, 4, 5, 4, \ldots]$	0.2299	0.2320	0.2306	0.3192	0.2319	0.3206	0.3177	0.3471	
$[0; 5, 5, 5, 5, \ldots]$	0.2465	0.2458	0.2461	0.3167	0.2455	0.3273	0.3121	0.3510	

Table 4 Exponent β_* in the blow-up of derivatives of the rotation number with respect to ε , for several rotation numbers and families

θ	Family (5)	Family (6	5)		Family (8)	Family (7)			
		$\kappa = 0.3$	$\kappa = 0.7$	$\kappa = 4/3$	$\kappa = 1/2$	$\kappa = 0.6$	$\kappa = 0.9$	$\kappa = 1.5$	
$[0; 1, 1, 1, 1, \dots]$	0.1562	0.1571	0.1566	0.2115	0.1564	0.2123	0.2370	0.2416	
$[0; 2, 1, 2, 1, \ldots]$	0.1789	0.1664	0.1786	0.2378	0.1786	0.2426	0.2612	0.3128	
$[0; 2, 2, 2, 2, \ldots]$	0.1645	0.1666	0.1665	0.2301	0.1663	0.2248	0.2254	0.2507	
$[0; 3, 1, 3, 1, \ldots]$	0.2048	0.2116	0.2064	0.2813	0.2111	0.2538	0.2428	0.3024	
$[0; 3, 2, 3, 2, \ldots]$	0.1851	0.1891	0.1809	0.2460	0.1780	0.2183	0.2254	0.2701	
$[0; 3, 3, 3, 3, \ldots]$	0.1871	0.1877	0.1877	0.2341	0.1881	0.2413	0.2552	0.2775	
$[0; 4, 1, 4, 1, \ldots]$	0.2484	0.2425	0.2425	0.2901	0.2326	0.2802	0.2938	0.3780	
$[0; 4, 2, 4, 2, \ldots]$	0.2152	0.2223	0.2188	0.2615	0.2105	0.2430	0.2567	0.2849	
$[0; 4, 3, 4, 3, \ldots]$	0.1947	0.2113	0.1950	0.2571	0.2026	0.2348	0.2436	0.3004	
$[0; 4, 4, 4, 4, \ldots]$	0.2146	0.2193	0.2175	0.2828	0.2174	0.2840	0.2753	0.3375	
$[0; 5, 1, 5, 1, \ldots]$	0.2794	0.2880	0.2874	0.3388	0.2814	0.3441	0.3257	0.3762	
$[0; 5, 2, 5, 2, \ldots]$	0.2214	0.2246	0.2396	0.2809	0.2224	0.2867	0.2829	0.3142	
$[0; 5, 3, 5, 3, \ldots]$	0.2347	0.2322	0.2358	0.2843	0.2306	0.2867	0.2866	0.3213	
$[0; 5, 4, 5, 4, \ldots]$	0.2349	0.2349	0.2386	0.3216	0.2411	0.3217	0.3162	0.3475	
$[0; 5, 5, 5, 5, \ldots]$	0.2468	0.2369	0.2446	0.3209	0.2416	0.3487	0.3201	0.3483	

and multiplying at both sides by $\alpha_{(n-1)}$ we obtain

$$\mathcal{R}_{n-1}[f_{\lambda}](\alpha_{(n-1)}h_{\lambda}(x)) \simeq \alpha_{(n-1)}h_{\lambda}(x+\theta^n).$$



Fig. 11 Arnold tongues corresponding to few hundreds of Diophantine rotation numbers for the Arnold family (5). As usual, we plot α in the horizontal axis and ε in the vertical axis

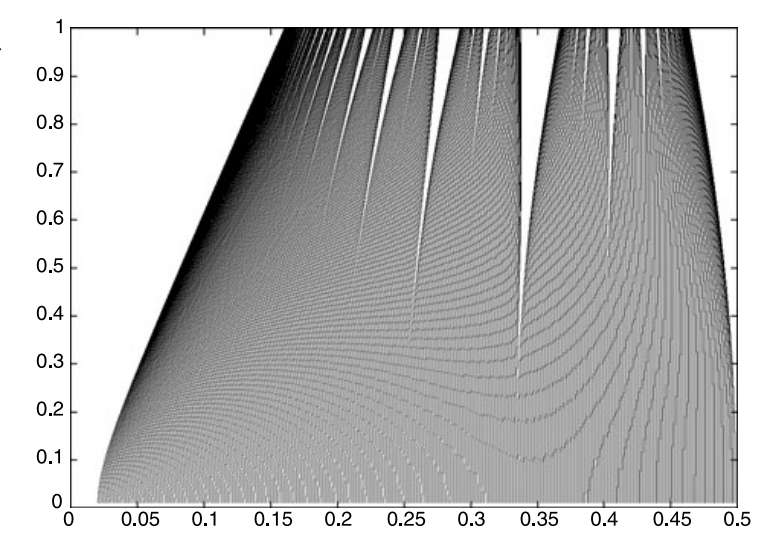
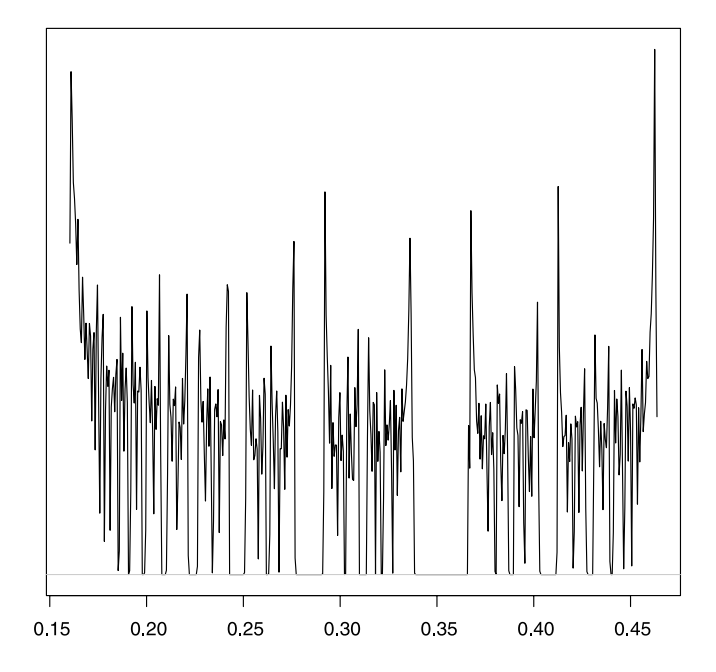


Fig. 12 Density distribution of the Arnold tongues at the critical point $\varepsilon = 1$. We do not include the vertical axis since the value depends on the smoothing parameters of the histogram, and this plot pretends to represent qualitatively that the density of the critical points becomes singular



Since $\lambda \simeq 0$ we can write $\mathcal{R}_{n-1}[f_{\lambda}] \simeq f_{\gamma^{n-1}\lambda}$ and, introducing the scaled variable $y = x/\theta^{n-1}$, we get an expression like (32) for the conjugacy $h_{\gamma\lambda}$ of $f_{\gamma\lambda}$ to a rotation.

In general, using (32) we compute $||h_{\gamma\lambda}||_r \simeq \alpha_* ||h_{\lambda}(\sigma \cdot)||_r = \sigma^{r-\frac{1}{2}} ||h_{\lambda}||_r$. Finally, introducing the first order of (31) into this relation for the norms, we conclude that

$$B_*(r) = -\left(r - \frac{1}{2}\right) \frac{\log \sigma}{\log \gamma} - \frac{\log \alpha_*}{\log \gamma},\tag{33}$$

and that P_* is log-periodic of period log γ .

For example, for a cubic family and fixing θ to be the golden mean, we have that $\sigma \simeq 0.61803...$ and $\gamma = \alpha^2 \simeq 1.66042...$, so that the slope of the affine expression (33) is expected to be $\simeq 0.949...$ This prediction agrees with our numerical experiments.

In the left plot of Fig. 14 we show the exponent $B_*(r)$ as a function of the index r for several families of circle maps (we take θ as the golden mean). We observe a very good agreement between maps of the same criticality. Similar results are obtained for the other



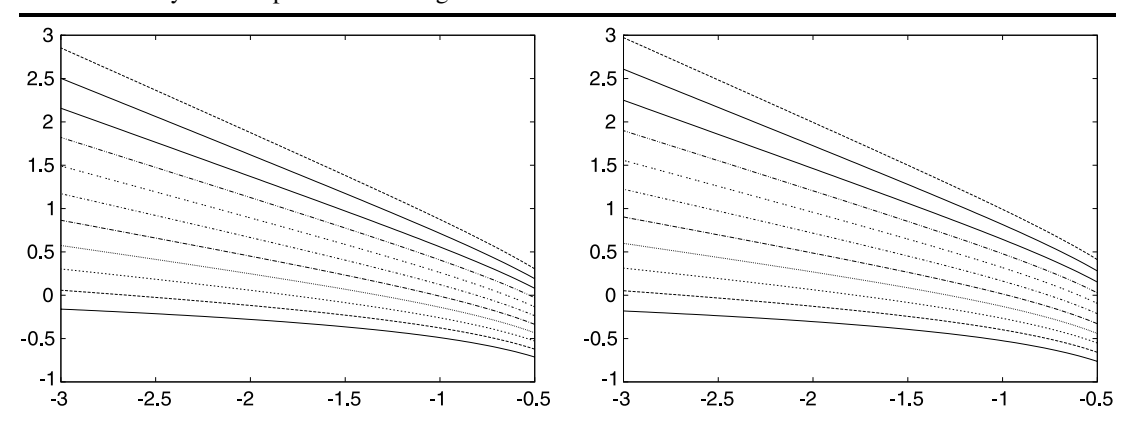


Fig. 13 Evolution of the *r*-Sobolev norm—for r = i/50, with i = 50, 55, 60, 65, 70, 75, 80, 85, 90, 95 and 100—of the conjugacy to a rotation along the Arnold tongue corresponding to $\theta = (\sqrt{5} - 1)/2$. *Left*: Family (5). *Right*: Family (6) with $\kappa = 4/3$

Table 5 Exponent $B_*(r)$ in expression (31)—for r = 67/50, 72/50 and 77/50—corresponding to the blow-up of the r-Sobolev norm of the conjugacy close to the critical point, for several rotation numbers and families

	Family	v (<mark>5</mark>)		Family (6), $\kappa = 0.3$			Family (6), $\kappa = 4/3$			Family (7), $\kappa = 0.6$		
θ r	67 50	$\frac{72}{50}$	$\frac{77}{50}$	67 50	$\frac{72}{50}$	$\frac{77}{50}$	67 50	$\frac{72}{50}$	$\frac{77}{50}$	67 50	$\frac{72}{50}$	77 50
$[0; 1, 1, \ldots]$	0.412	0.510	0.606	0.419	0.508	0.605	0.366	0.428	0.496	0.364	0.431	0.499
$[0; 2, 1, \ldots]$	0.433	0.527	0.623	0.431	0.526	0.622	0.383	0.450	0.534	0.390	0.457	0.529
$[0; 2, 2, \ldots]$	0.420	0.515	0.612	0.423	0.515	0.612	0.373	0.439	0.505	0.376	0.442	0.513
$[0; 3, 1, \ldots]$	0.459	0.559	0.661	0.462	0.562	0.663	0.408	0.478	0.551	0.406	0.479	0.552
$[0; 3, 2, \ldots]$	0.437	0.526	0.626	0.437	0.530	0.624	0.390	0.463	0.521	0.393	0.460	0.526
$[0; 3, 3, \ldots]$	0.429	0.529	0.625	0.435	0.532	0.623	0.383	0.455	0.518	0.385	0.451	0.514
$[0; 4, 1, \ldots]$	0.494	0.595	0.701	0.491	0.593	0.702	0.439	0.522	0.597	0.436	0.524	0.595
$[0; 4, 2, \ldots]$	0.455	0.550	0.649	0.455	0.548	0.643	0.434	0.484	0.551	0.434	0.491	0.565
$[0; 4, 3, \ldots]$	0.446	0.543	0.643	0.442	0.532	0.624	_	_	_	_	_	_
$[0; 4, 4, \ldots]$	0.447	0.543	0.648	0.443	0.538	0.636	_	_	_	_	_	_
$[0; 5, 1, \ldots]$	0.522	0.625	0.739	0.520	0.628	0.741	_	_	_	_	_	_
$[0; 5, 2, \ldots]$	0.474	0.566	0.660	0.475	0.573	0.663	_	_	_	_	_	_
$[0; 5, 3, \ldots]$	0.466	0.562	0.658	0.468	0.561	0.657	_	_	_	_	_	_
$[0; 5, 4, \ldots]$	0.468	0.563	0.664	0.466	0.567	0.665	_	_	_	_	_	_
$[0; 5, 5, \ldots]$	0.479	0.572	0.680	0.475	0.575	0.674	-	_	_	-	_	_

selected quadratic rotation numbers. In addition, in the right plot of Fig. 14 we illustrate the periodic correction predicted by the renormalization group (see details in the caption).

6.3 Relation of the Blow up Exponents with Brjuno Function

In previous sections we have characterized the first asymptotic exponents in the blow up of the derivatives of the rotation number (see Sect. 6.1) and the r-Sobolev regularity of the conjugation to a rotation (see Sect. 6.2). It turns out that—given a certain family—these exponents depend on the arithmetic properties of the rotation number. However, looking at formula (33), we have little intuition on this dependence since σ and γ depend on θ in a very complicated way.



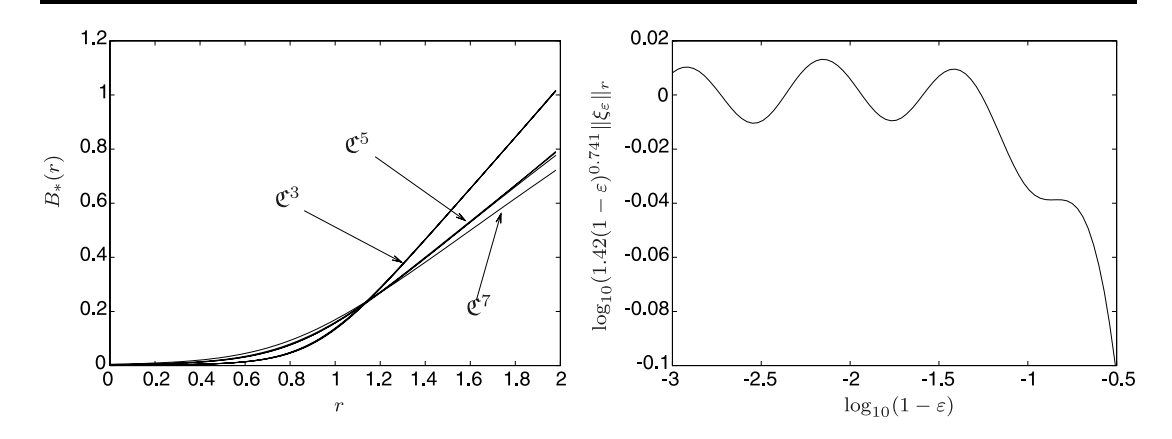


Fig. 14 Left: we plot $r \mapsto B_*(r)$, where $B_*(r)$ is the exponent in the expression (31), corresponding to the blow-up of the r-Sobolev norm of the conjugacy close to the critical point for the golden mean $\theta = (\sqrt{5}-1)/2$ and the Families (5), (6) for $\kappa = 0.3, 0.7, 4/3$, (7) for $\kappa = 0.6, 0.9, 1.5$ and (8) for $\kappa = 0.5$. Right: we plot $\log_{10}(1-\varepsilon) \mapsto \log_{10}(1.42(1-\varepsilon)^{0.741} \|\xi_{\varepsilon}\|_r)$, for $\theta = [0; 5, 1, 5, 1, \ldots]$, corresponding to Family (6) with $\kappa = 0.3$ and r = 77/50. The coefficients 1.42 and 0.741 correspond to subtract the linear fit in $\log_{10} - \log_{10} \sin(\theta)$

In order to study the dependence of the exponents β_* and $B_*(r)$ on the rotation number, we make use of the Brjuno function, which measures how much Diophantine a number is. Brjuno function can be computed recursively using the following formula

$$\mathcal{B}(\theta) = -\log \theta + \theta \mathcal{B}(\theta^{-1}), \quad \theta \in (0, 1). \tag{34}$$

Firstly, in Fig. 15 we plot $\mathcal{B}(\theta) \mapsto \beta_*$ for several of the studied families. It seems that the exponent β_* is larger when the Brjuno function increases (i.e., when the rotation number is "closer" to be a rational number), and that this behavior is organized in families. In all cases we obtain an upper boundary curve which is given by the rotation numbers $\theta = [0; 2, 2, \ldots], [0; 3, 3, \ldots], [0; 4, 4, \ldots]$ and $[0; 5, 5, \ldots]$, respectively. On the other hand, we observe a lower boundary curve that corresponds to the rotation numbers $\theta = [0; 1, 1, \ldots], [0; 2, 1, \ldots], [0; 3, 2, \ldots], [0; 4, 2, \ldots], [0; 3, 1, \ldots], [0; 5, 2, \ldots], [0; 4, 1, \ldots]$ and $[0; 5, 1, \ldots], [0; 5, 2, \ldots], [0; 4, 1, \ldots]$ and $[0; 5, 1, \ldots], [0; 5, 2, \ldots], [0; 4, 1, \ldots]$ and $[0; 5, 1, \ldots], [0; 5, 2, \ldots], [0$

Secondly, in Fig. 16 we consider the exponent $B_*(r)$ in the blow up of the r-Sobolev norm. The behavior observed is very similar to that of the exponents of the blow-up of the derivatives of the rotation number with respect to parameters. Analogous results have been obtained for the other families studied in this paper.

7 Conclusions

In this study we have used two numerical methods to compute very accurately Arnold tongues, given by curves $\omega(\varepsilon)$, as well as the corresponding derivatives $\omega'(\varepsilon)$. We have found that the methods work reliably and efficiently even close to the values of ε where the circle maps cease to be diffeomorphisms and the conjugacies of the circle maps to a rigid rotation cease to be smooth.

This allows us to extrapolate with confidence to the breakdown and to uncover some new phenomena. Our main findings are:

1. We have found that the Arnold tongues remain finitely differentiable at the blow up and we have found the optimal regularity. Indeed, Arnold tongues are at least $C^{1+\alpha}$, α being a universal number. For the golden mean case, the curve is in fact smoother than C^2 .



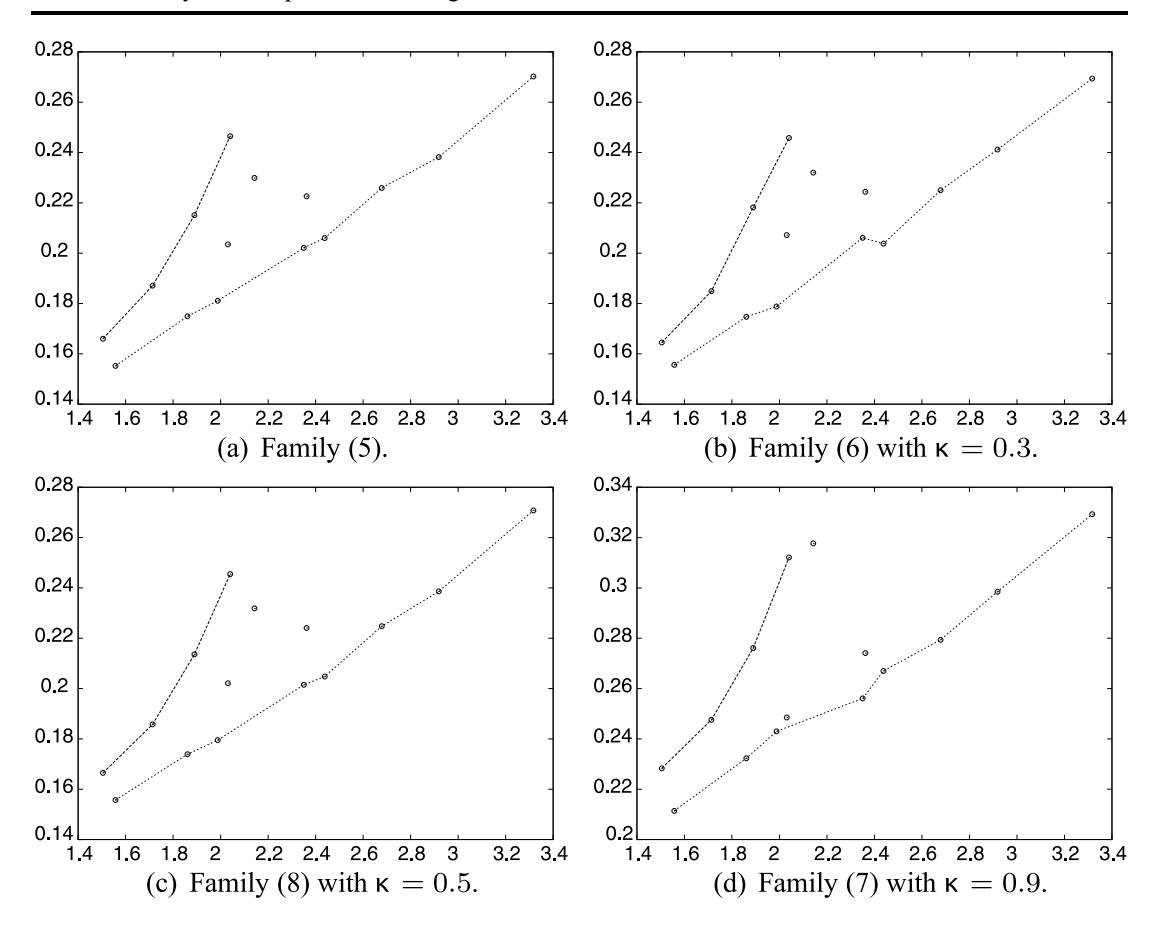


Fig. 15 We show $\mathcal{B}(\omega) \mapsto \beta_*$, where $\mathcal{B}(\theta)$ is the Brjuno function—computed using (34)—and β_* is the exponent in the blow-up of derivatives of the rotation number with respect to ω —introduced in (30). The *upper boundary* curve corresponds to $\theta = [0; 2, 2, \ldots], [0; 3, 3, \ldots], [0; 4, 4, \ldots]$ and $[0; 5, 5, \ldots]$, respectively. The *lower boundary curve* corresponds to $\theta = [0; 1, 1, \ldots], [0; 2, 1, \ldots], [0; 3, 2, \ldots], [0; 4, 2, \ldots], [0; 3, 1, \ldots], [0; 5, 2, \ldots], [0; 4, 1, \ldots]$ and $[0; 5, 1, \ldots]$, respectively

- 2. We have found that Sobolev norms of the conjugacy to rotations blow up as powers. The exponents of the blow up are also universal numbers and they depend affinely on the index of the Sobolev space. We have found also log-periodic corrections to the scalings and we show that these corrections are predicted by the renormalization group.
- 3. The exponents of blow up of several quantities are related to the Brjuno function of the corresponding rotation number.

Given the analogy between breakdown of smooth conjugacies and phase transitions, we present renormalization group explanations of (1) and (2) which give quantitative agreement (about to 3 figures) with the computed numerically exponents. The observation (3) remains a challenge for theoretical explanations.

As we mentioned in the introduction, we have presented a renormalization group picture at the level of rigor of theoretical physics. The task of formulating this picture at the level of full mathematical rigor will have to be postponed for future work. In addition, this picture should the adapted in order to deal with general Diophantine (or Bruno) numbers rather than just Diophantine numbers having periodic continued fraction.

Acknowledgements The authors have been partially supported by the MCyT-FEDER grant MTM2009-06973. The work of R.L. has been partially supported by NSF grant DMS 0901389 and NHRP 0223 and A.L. has been supported by the fellowship PTA2008-1693-P. Moreover, A.L. also thanks the hospitality of



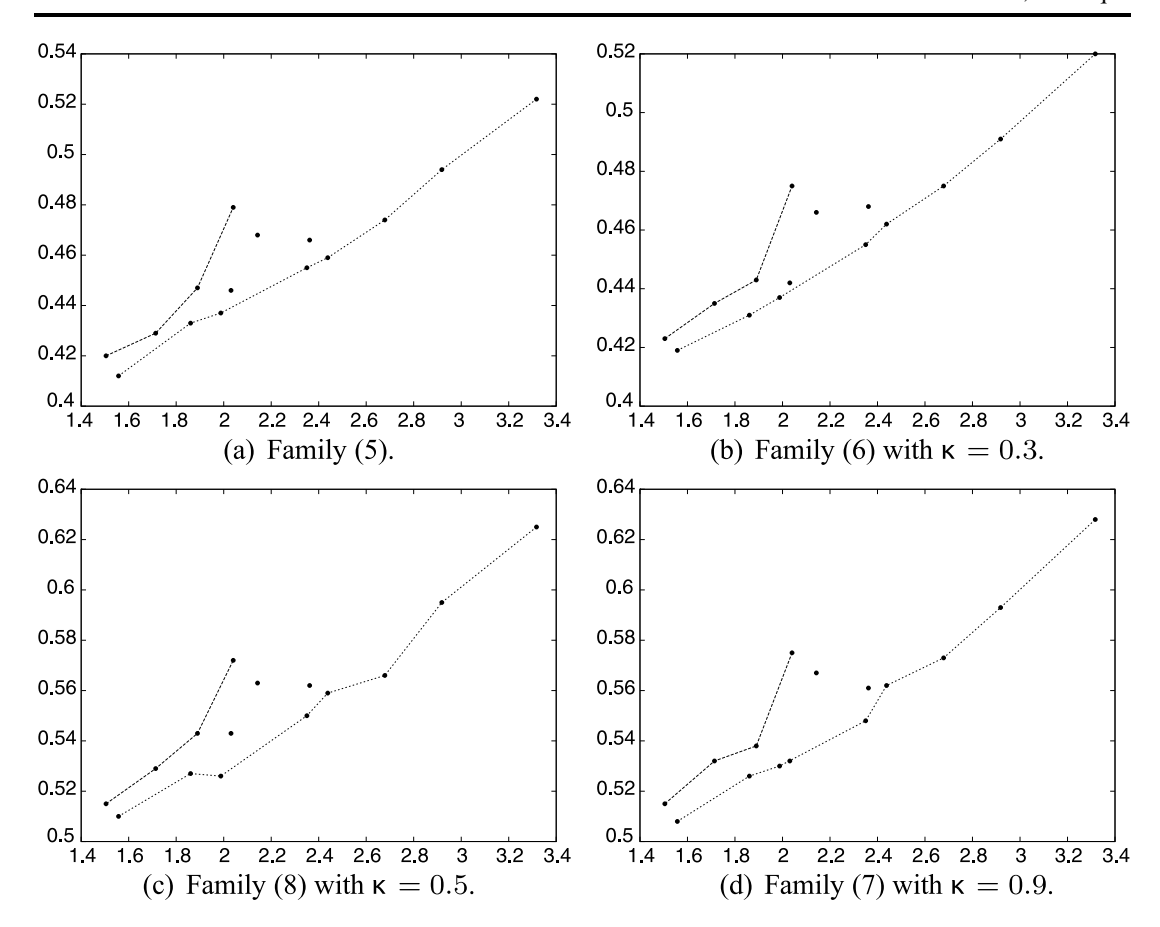


Fig. 16 We show $\mathcal{B}(\omega) \mapsto B_*(r)$, where $\mathcal{B}(\theta)$ is the Brjuno function (see text for details) and $B_*(r)$ is the exponent in the blow-up of r-Sobolev norm of the conjugation. The *upper boundary curve* corresponds to $\theta = [0; 2, 2, \ldots], [0; 3, 3, \ldots], [0; 4, 4, \ldots]$ and $[0; 5, 5, \ldots]$, respectively. The *lower boundary curve* corresponds to $\theta = [0; 1, 1, \ldots], [0; 2, 1, \ldots], [0; 3, 2, \ldots], [0; 4, 2, \ldots], [0; 3, 1, \ldots], [0; 5, 2, \ldots], [0; 4, 1, \ldots]$ and $[0; 5, 1, \ldots]$, respectively

the Department of Mathematics at U. of Texas at Austin during part of the development of this work. Finally, we wish to thank Renato Calleja, Nikola Petrov and Jordi Villanueva for interesting discussions.

References

- Arnold, V.I.: Small denominators. I. Mapping the circle onto itself. Izv. Akad. Nauk SSSR, Ser. Mat. 25, 21–86 (1961)
- 2. Calleja, R., de la Llave, R.: Fast numerical computation of quasi-periodic equilibrium states in 1-D statistical mechanics. Nonlinearity **22**(1), 1311–1336 (2009)
- 3. Cabré, X., Fontich, E., de la Llave, R.: The parameterization method for invariant manifolds. I. Manifolds associated to non-resonant subspaces. Indiana Univ. Math. J. **52**(2), 283–328 (2003)
- 4. Cabré, X., Fontich, E., de la Llave, R.: The parameterization method for invariant manifolds. III. Overvie w and applications. J. Differ. Equ. **218**(2), 444–515 (2005)
- 5. Díaz-Espinosa, O., de la Llave, R.: Renormalization and central limit theorem for critical dynamical systems with weak external noise. J. Mod. Dyn. 1(3), 477–543 (2007)
- 6. Díaz-Espinosa, O., de la Llave, R.: Renormalization of arbitrary weak noises for one-dimensional critical dynamical systems: summary of results and numerical explorations. In: Holomorphic Dynamics and Renormalization. Fields Inst. Commun., vol. 53, pp. 331–359. Am. Math. Soc. Providence (2008)
- 7. Denjoy, A.: Sur les courbes définies par les équations différentielles à la surface du tore. J. Math. Pures Appl. (9) 11, 333–375 (1932)
- 8. de Faria, E.: Asymptotic rigidity of scaling ratios for critical circle mappings. Ergod. Theory Dyn. Syst. **19**(4), 995–1035 (1999)



- 9. de Faria, E., de Melo, W.: Rigidity of critical circle mappings. I. J. Eur. Math. Soc. 1(4), 339–392 (1999)
- 10. de Faria, E., de Melo, W.: Rigidity of critical circle mappings. II. J. Am. Math. Soc. **13**(2), 343–370 (2000)
- 11. de la Llave, R.: Invariant manifolds associated to nonresonant spectral subspaces. J. Stat. Phys. **87**(1–2), 211–249 (1997)
- 12. de la Llave, R.: A tutorial on KAM theory. In: Smooth Ergodic Theory and Its Applications, Seattle, WA, 1999. Proc. Sympos. Pure Math., vol. 69, pp. 175–292. Am. Math. Soc, Providence (2001)
- 13. de la Llave, R., Wayne, C.E.: On Irwin's proof of the pseudostable manifold theorem. Math. Z. **219**(2), 301–321 (1995)
- 14. de la Llave, R., Huguet, G., Sire, Y.: Fast numerical algorithms for the computation of invariant tori in Hamiltonian systems. Preprint available electronically at http://www.ma.utexas.edu/mp_arc-bin/mpa?yn=09-2
- 15. de la Llave, R., Petrov, N.P.: Theory of circle maps and the problem of one-dimensional optical resonator with a periodically moving wall. Phys. Rev. E **59**(6), 6637–6651 (1999)
- 16. de la Llave, R., Petrov, N.P.: Regularity of conjugacies between critical circle maps: an experimental study. Exp. Math. **11**(2), 219–241 (2002)
- 17. de Melo, W., van Strien, S.: One-Dimensional Dynamics. Ergeb. Math. Grenzgeb. (3) [Results in Mathematics and Related Areas (3)], vol. 25. Springer, Berlin (1993)
- 18. Epstein, H.: Fixed points of composition operators. II. Nonlinearity 2(2), 305–310 (1989)
- 19. Feigenbaum, M.J.: Quantitative universality for a class of nonlinear transformations. J. Stat. Phys. **19**(1), 25–52 (1978)
- 20. Fenichel, N.: Asymptotic stability with rate conditions. Indiana Univ. Math. J. 23, 1109–1137 (1973/74)
- 21. Feigenbaum, M.J., Kadanoff, L.P., Shenker, S.J.: Quasiperiodicity in dissipative systems: a renormalization group analysis. Physica D 5(2–3), 370–386 (1982)
- 22. Glass, L.: Cardiac arrhythmias and circle maps—a classical problem. Chaos 1(1), 13–19 (1991)
- Graczyk, J., Świątek, G.: Critical circle maps near bifurcation. Commun. Math. Phys. 176(2), 227–260 (1996)
- Herman, M.R.: Sur la conjugaison différentiable des difféomorphismes du cercle à des rotations. Publ. Math. Inst. Hautes Études Sci. 49, 5–233 (1979)
- Heiberger, R.M., Holland, B.: Statistical Analysis and Data Display: An Intermediate Course with Examples in S-Plus, R, and SAS. Springer Texts in Statistics. Springer, Berlin (2004). 0-387-40270-5
- 26. Hida, Y., Li, X., Bailey, D.H.: QD (quad-double/double-double computation package). Available electronically at http://crd.lbl.gov/dhbailey/mpdist/ (2005)
- Ignatov, A.M.: Trivelpiece-Gould modes in a corrugated plasma slab. Phys. Rev. E 51(2), 1391–1399 (1995)
- 28. Jorba, À., Olmedo, E.: On the computation of reducible invariant tori on a parallel computer. SIAM J. Appl. Dyn. Syst. **8**(4), 1382–1404 (2009)
- 29. Katok, A., Hasselblatt, B.: Introduction to the Modern Theory of Dynamical Systems. Encycl. Math. Appl., vol. 54. Cambridge University Press, Cambridge (1995)
- 30. Katznelson, Y., Ornstein, D.S.: The differentiability of the conjugation of certain diffeomorphisms of the circle. Ergod. Theory Dyn. Syst. **9**(4), 643–680 (1989)
- 31. Khanin, K.M., Sinaĭ, Ya.G.: A new proof of M. Herman's theorem. Commun. Math. Phys. **112**(1), 89–101 (1987)
- 32. Khanin, K., Teplinsky, A.: Herman's theory revisited. Invent. Math. 178(2), 333–344 (2009)
- 33. Lanford III, O.E.: Functional equations for circle homeomorphisms with golden ratio rotation number. J. Stat. Phys. **34**(1–2), 57–73 (1984)
- 34. Lanford III, O.E., de la Llave, R.: Solution of the functional equation for critical circle mappings with golden rotation number. Manuscript
- 35. Luque, A., Villanueva, J.: Computation of derivatives of the rotation number for parametric families of circle diffeomorphisms. Physica D **237**(20), 2599–2615 (2008)
- 36. Mestel, B.: A computer assisted proof of universality for cubic critical maps of the circle with golden mean rotation number. PhD thesis, University of Warwick (1984)
- 37. Moser, J.: A rapidly convergent iteration method and non-linear differential equations. II. Ann. Sc. Norm. Super. Pisa, Cl. Sci. (3) **20**, 499–535 (1966)
- 38. Moser, J.: A rapidly convergent iteration method and non-linear partial differential equations. I. Ann. Sc. Norm. Super. Pisa, Cl. Sci. (3) **20**, 265–315 (1966)
- 39. Moser, J., Pöschel, J.: An extension of a result by Dinaburg and Sinaĭon quasiperiodic potentials. Comment. Math. Helv. **59**(1), 39–85 (1984)
- 40. Östlund, S., Rand, D., Sethna, J., Siggia, E.: Universal properties of the transition from quasiperiodicity to chaos in dissipative systems. Physica D 8(3), 303–342 (1983)



- 41. Poincaré, H.: Sur les courbes définies par les équations différentielles. J. Math. Pures Appl. 1, 167–244 (1885)
- Pommeau, Y., Maneville, P.: Intermittent transition to turbulence in dissipative dynamical systems. Commun. Math. Phys. 74(2), 189–197 (1980)
- 43. Risler, E.: Linéarisation des perturbations holomorphes des rotations et applications. Mém. Soc. Math. Fr. (N.S.) 77, viii+102 (1999)
- 44. Rüssmann, H.: On optimal estimates for the solutions of linear partial differential equations of first order with constant coefficients on the torus. In: Dynamical Systems, Theory and Applications, Rencontres, Battelle Res. Inst., Seattle, Wash., 1974. Lecture Notes in Phys., vol. 38, pp. 598–624. Springer, Berlin (1975)
- 45. Schaefer, H.: Topological vector spaces. In: Graduate Texts in Mathematics, vol. 3. Springer, New York (1971). Third printing corrected
- Seara, T.M., Villanueva, J.: On the numerical computation of Diophantine rotation numbers of analytic circle maps. Physica D 217(2), 107–120 (2006)
- 47. Shenker, S.J.: Scaling behavior in a map of a circle onto itself: empirical results. Physica D 5(2-3), 405-411 (1982)
- 48. Shraiman, B.I.: Transition from quasiperiodicity to chaos: a perturbative renormalization-group approach. Phys. Rev. A **29**(6), 3464–3466 (1984)
- Sinaĭ, Y.G., Khanin, K.M.: Renormalization group method in the theory of dynamical systems. Int. J. Mod. Phys. B 2(2), 147–165 (1988)
- 50. Sinaĭ, Y.G., Khanin, K.M.: Smoothness of conjugacies of diffeomorphisms of the circle with rotations. Usp. Mat. Nauk **44**(1(265)), 57–82, 247 (1989)
- 51. Świątek, G.: Rational rotation numbers for maps of the circle. Commun. Math. Phys. **119**(1), 109–128 (1988)
- 52. Tresser, C., Coullet, P.: Itérations d'endomorphismes et groupe derenormalisation. C. R. Acad. Sci. Paris Sér. A–B **287**(7), A577–A580 (1978)
- Vano, J.: A Nash-Moser implicit function theorem with Whitney regularity and applications. PhD thesis, University of Texas at Austin. Available electronically at http://hdl.handle.net/2152/655 (2002)
- 54. Yampolsky, M.: Hyperbolicity of renormalization of critical circle maps. Publ. Math. Inst. Hautes Études Sci. **96**, 1–41 (2003), 2002
- 55. Yampolsky, M.: Renormalization horseshoe for critical circle maps. Commun. Math. Phys. **240**(1–2), 75–96 (2003)
- 56. Yoccoz, J.-C.: Conjugaison différentiable des difféomorphismes du cercle dont le nombre de rotation vérifie une condition diophantienne. Ann. Sci. École Norm. Sup. (4) **17**(3), 333–359 (1984)
- 57. Yoccoz, J.C.: Il n'y a pas de contre-exemple de Denjoy analytique. C. R. Acad. Sci. Paris Sér. I Math. **298**(7), 141–144 (1984)
- 58. Yoccoz, J.-C.: Analytic linearization of circle diffeomorphisms. In: Dynamical Systems and Small Divisors, Cetraro, 1998. Lecture Notes in Math., vol. 1784, pp. 125–173. Springer, Berlin (2002)
- 59. Zehnder, E.: Generalized implicit function theorems with applications to some small divisor problems. I. Commun. Pure Appl. Math. **28**, 91–140 (1975)
- 60. Zehnder, E.: Generalized implicit function theorems with applications to some small divisor problems. II. Commun. Pure Appl. Math. **29**(1), 49–111 (1976)

